Solving $\mathrm{SU}(3)$ Yang-Mills theory on the lattice: a calculation of selected gauge observables with gradient flow

Hans Mathias Mamen Vege
04.07.19

Supervisor: *Andrea Shindler*
Co-supervisor: *Morten Hjorth-Jensen*

University of Oslo

The four forces of nature

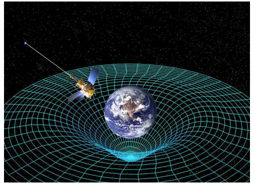

Gravity

The four forces of nature

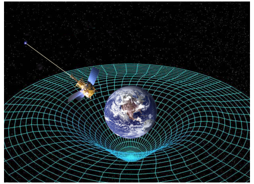

Gravity

Electromagnetism

The four forces of nature

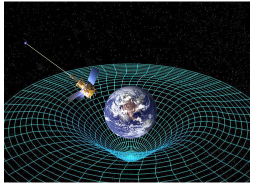

Gravity

Electromagnetism

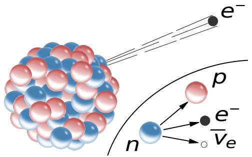

Weak nuclear force

The four forces of nature

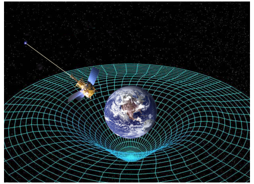

Gravity

Electromagnetism

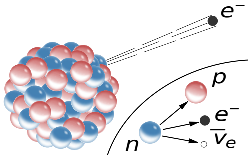

Weak nuclear force

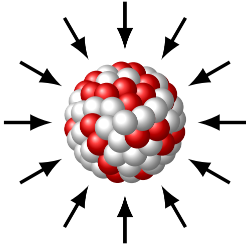

Strong nuclear force

What is the strong force?

Consists of:

- 6 quark flavors: up, down, strange, charm, bottom and top

The mass discrepancy is due to the interaction energy in which gluons are mediators.

What is the strong force?

Consists of:

- 6 quark flavors: up, down, strange, charm, bottom and top
- 8 gluons

The mass discrepancy is due to the interaction energy in which gluons are mediators.

What is the strong force?

Consists of:

- 6 quark flavors: up, down, strange, charm, bottom and top
- 8 gluons

The mass discrepancy is due to the interaction energy in which gluons are mediators.

What is the strong force?

Consists of:

- 6 quark flavors: up, down, strange, charm, bottom and top
- 8 gluons

A **proton** consists of: up-, up- and down-quarks

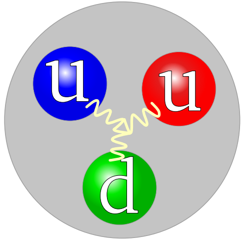

The mass discrepancy is due to the interaction energy in which gluons are mediators.

What is the strong force?

Consists of:

- 6 quark flavors: up, down, strange, charm, bottom and top
- 8 gluons

A **proton** consists of: up-, up- and down-quarks
Mass discrepancy:

$$m_p \neq m_u + m_u + m_d,$$

$$936 \text{ MeV} \neq 3 \text{ MeV} + 3 \text{ MeV} + 6 \text{ MeV}.$$

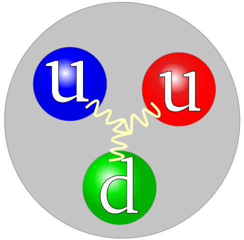

The mass discrepancy is due to the interaction energy in which gluons are mediators.

Comparing the strong force and QED

QED Quantum Electrodynamics(Electromagnetism), a U(1) theory:

$$\mathcal{L}_{\text{QED}} = \sum_{f=\text{fermions}} \bar{\psi}_f(i\gamma^\mu(\partial_\mu + ieQ_f A_\mu) - m_f)\psi_f - \frac{1}{4}F_{\mu\nu}F^{\mu\nu}$$

Field strength tensor:

$$F_{\mu\nu} = \partial_\mu A_\nu - \partial_\nu A_\mu$$

e is the coupling constant and Q_f is the charge.

Comparing the strong force and QED

QED Quantum Electrodynamics(Electromagnetism), a $\mathrm{U}(1)$ theory:

$$\mathcal{L}_{\text{QED}} = \sum_{f=\text{fermions}} \bar{\psi}_f(i\gamma^\mu(\partial_\mu + ieQ_f A_\mu) - m_f)\psi_f - \frac{1}{4}F_{\mu\nu}F^{\mu\nu}$$

Field strength tensor:

$$F_{\mu\nu} = \partial_\mu A_\nu - \partial_\nu A_\mu$$

The strong nuclear force, QCD, a $\mathrm{SU}(3)$ theory:

$$\mathcal{L}_{\text{QCD}} = \sum_{f=u,d,\ldots} \bar{\psi}_f(i\gamma^\mu(\partial_\mu + ig_S A^a_\mu T^a) - m_f)\psi_f - \frac{1}{4}F^a_{\mu\nu}F^{a\mu\nu}$$

Field strength tensor:

$$F_{\mu\nu} = \partial_\mu A^a_\nu - \partial_\nu A^a_\mu - g_S f^{abc} A^b_\mu A^c_\nu$$

e is the coupling constant and Q_f is the charge.

Why is the strong force strong?

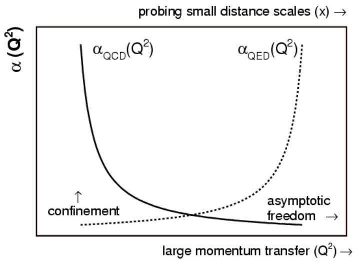

https://www-cdf.fnal.gov/~group/WORK/DISS_PAGE/diss_page.htm

Coupling constant α strength of the force in an interaction.

- In physics, **a coupling constant** or gauge coupling parameter (or, more simply, a coupling), is a number that determines the strength of the force exerted in an interaction.

Why is the strong force strong?

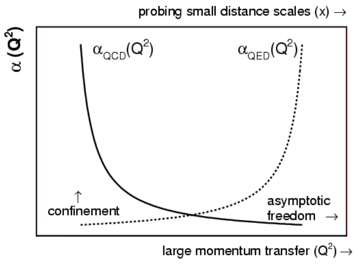

https://www-cdf.fnal.gov/~group/WORK/DISS_PAGE/diss_page.htm

Coupling constant α strength of the force in an interaction.

- $\alpha_G \approx 1.75 \times 10^{-45}$

- In physics, **a coupling constant** or gauge coupling parameter (or, more simply, a coupling), is a number that determines the strength of the force exerted in an interaction.

Why is the strong force strong?

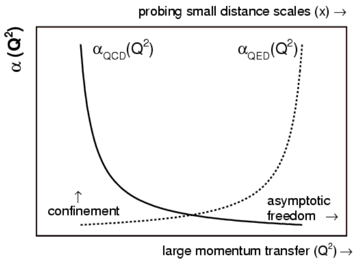

https://www-cdf.fnal.gov/~group/WORK/DISS_PAGE/diss_page.htm

Coupling constant α strength of the force in an interaction.

- $\alpha_G \approx 1.75 \times 10^{-45}$
- $\alpha_W \approx 10^{-6} - 10^{-7}$

- In physics, **a coupling constant** or gauge coupling parameter (or, more simply, a coupling), is a number that determines the strength of the force exerted in an interaction.

Why is the strong force strong?

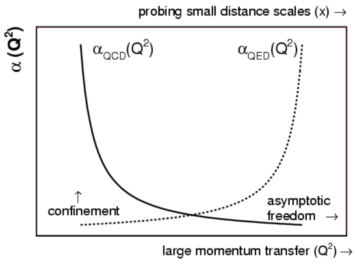

https://www-cdf.fnal.gov/~group/WORK/DISS_PAGE/diss_page.htm

Coupling constant α strength of the force in an interaction.

- $\alpha_G \approx 1.75 \times 10^{-45}$
- $\alpha_W \approx 10^{-6} - 10^{-7}$
- $\alpha_{\mathrm{QED}} \approx \frac{1}{137} \approx 0.0073$

- In physics, **a coupling constant** or gauge coupling parameter (or, more simply, a coupling), is a number that determines the strength of the force exerted in an interaction.

Why is the strong force strong?

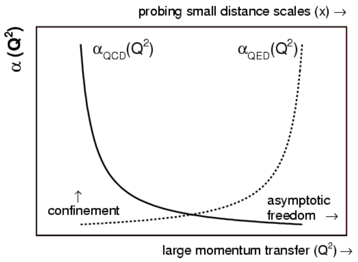

https://www-cdf.fnal.gov/~group/WORK/DISS_PAGE/diss_page.htm

Coupling constant α strength of the force in an interaction.

- $\alpha_G \approx 1.75 \times 10^{-45}$
- $\alpha_W \approx 10^{-6} - 10^{-7}$
- $\alpha_{\text{QED}} \approx \frac{1}{137} \approx 0.0073$
- $\alpha_S \approx \frac{g_S^2}{4\pi} \approx 1$

- In physics, **a coupling constant** or gauge coupling parameter (or, more simply, a coupling), is a number that determines the strength of the force exerted in an interaction.
- **Couplings at low energy.**

Why is the strong force strong?

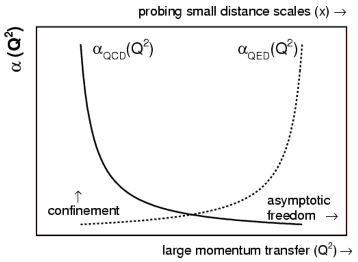

https://www-cdf.fnal.gov/~group/WORK/DISS_PAGE/diss_page.htm

Coupling constant α strength of the force in an interaction.

- $\alpha_G \approx 1.75 \times 10^{-45}$
- $\alpha_W \approx 10^{-6} - 10^{-7}$
- $\alpha_{\mathrm{QED}} \approx \frac{1}{137} \approx 0.0073$
- $\alpha_S \approx \frac{g_S^2}{4\pi} \approx 1$

Can't use perturbation theory on strong force in low-energy regime!

- In physics, **a coupling constant** or gauge coupling parameter (or, more simply, a coupling), is a number that determines the strength of the force exerted in an interaction.
- **Couplings at low energy.**
- We cannot make **perturbative expansions** in the low-energy regime of the strong nuclear force.
- Which is really a shame, since many interesting phenomena such as **confinement** is a low-energy phenomena.

Why is the strong force strong?

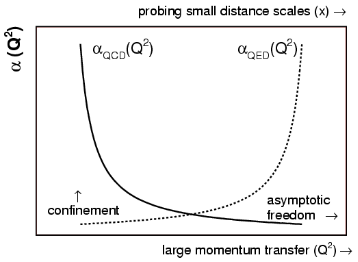

https://www-cdf.fnal.gov/~group/WORK/DISS_PAGE/diss_page.htm

Coupling constant α strength of the force in an interaction.

- $\alpha_G \approx 1.75 \times 10^{-45}$
- $\alpha_W \approx 10^{-6} - 10^{-7}$
- $\alpha_{\text{QED}} \approx \frac{1}{137} \approx 0.0073$
- $\alpha_S \approx \frac{g_S^2}{4\pi} \approx 1$

Can't use perturbation theory on strong force in low-energy regime!

- In physics, **a coupling constant** or gauge coupling parameter (or, more simply, a coupling), is a number that determines the strength of the force exerted in an interaction.
- **Couplings at low energy.**
- We cannot make **perturbative expansions** in the low-energy regime of the strong nuclear force.
- Which is really a shame, since many interesting phenomena such as **confinement** is a low-energy phenomena.

Confinement: a low-energy phenomena

No free color charges in nature!

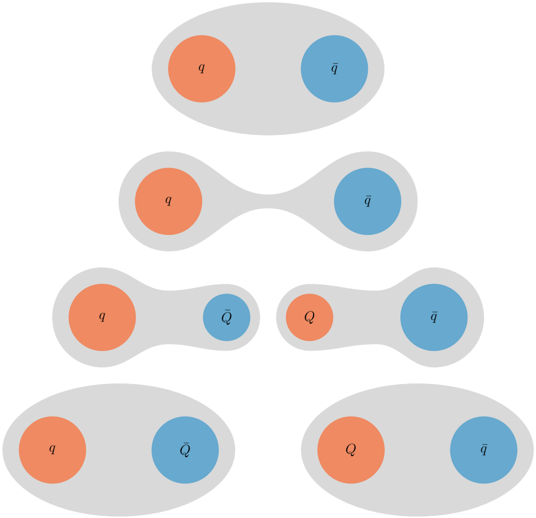

If we try to pull apart **two quarks in a meson**, more and more energy is required until we have enough energy to spontaneously create a **quark-antiquark** pair, forming thus **two new mesons.**

QCD and nuclear physics

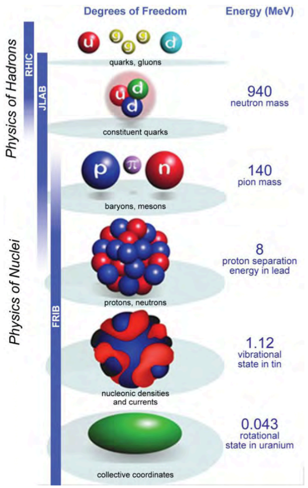

FRIB Users Organization for the NSAC Long Range Plan Implementation Subcommittee

Need to understand the low-energy regime in order to better understand nuclear physics!

The most fundamental theory we currently have of nuclear physics is QCD. Understanding QCD will help us understand nuclear physics and more *emergent* theories. But to bridge the gaps between these theories is difficult, as QCD contains a large number of degrees of freedom. Thus, a numerical approach is needed.

QCD and nuclear physics

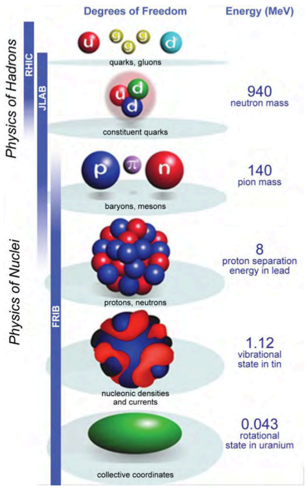

FRIB Users Organization for the NSAC Long Range Plan Implementation Subcommittee

Need to understand the low-energy regime in order to better understand nuclear physics!
→ numerical methods(e.g. lattice QCD)

The most fundamental theory we currently have of nuclear physics is QCD. Understanding QCD will help us understand nuclear physics and more *emergent* theories. But to bridge the gaps between these theories is difficult, as QCD contains a large number of degrees of freedom. Thus, a numerical approach is needed.

How we measure: path integrals

Going from t_0 at A to a time t_1 at B can be given in terms of a path integral.

How we measure: path integrals

Going from t_0 at A to a time t_1 at B can be given in terms of a path integral.

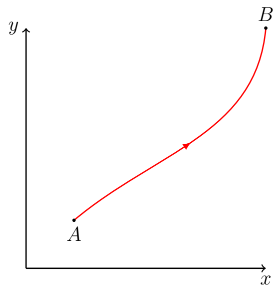

Classically, only one possible path obtained from the principle of least action.

- Classically we only have one available path given to us from the principle of least action.

How we measure: path integrals

Going from t_0 at A to a time t_1 at B can be given in terms of a path integral.

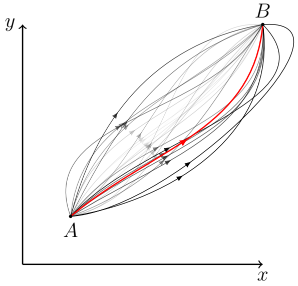

In quantum mechanics, there is lots of possible paths.

- Classically we only have one available path given to us from the principle of least action.
- In quantum mechanics, we have several available paths, which are all weighted by some probability amplitude.

How we measure: path integrals

Going from t_0 at A to a time t_1 at B can be given in terms of a path integral.

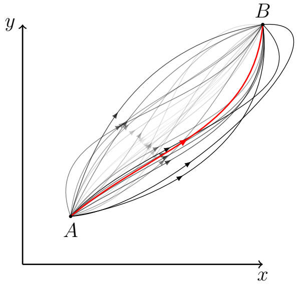

In quantum mechanics, there is lots of possible paths.
Principle of least action (or stationary condition): $\frac{\delta}{\delta x(t)}\left(S\left[x(t)\right]\right) = 0$

- Classically we only have one available path given to us from the principle of least action.
- In quantum mechanics, we have several available paths, which are all weighted by some probability amplitude.

How we measure: path integrals

Going from t_0 at A to a time t_1 at B can be given in terms of a path integral.

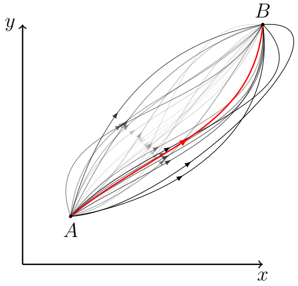

In quantum mechanics, there is lots of possible paths.
Principle of least action (or stationary condition):
$\frac{\delta}{\delta x(t)}\left(S\left[x(t)\right]\right) = 0$*Sum over all possible paths $\rightarrow$ the most likely path.*

- Classically we only have one available path given to us from the principle of least action.
- In quantum mechanics, we have several available paths, which are all weighted by some probability amplitude.

Path integrals

Given a field ϕ^M in Minkowski space, the *partition function* Z is given by

$$
\begin{aligned}
Z &= \int \mathcal{D}\phi^M \mathrm{e}^{\frac{i}{\hbar} S^M[\phi^M]} \\
&\downarrow \quad \hbar = 1, \quad \tau \to -it \qquad \text{imaginary time(euclidean space)!} \\
&= \int \mathcal{D}\phi \mathrm{e}^{-S[\phi]}
\end{aligned}
$$

where $\mathcal{D}$ is an integration of all possible paths in space.

- We go to imaginary time in order to avoid oscillations due to the complex phase.
- We must also change S so it is in Euclidean space.

Path integrals

Given a field ϕ^M in Minkowski space, the *partition function* Z is given by

$$
\begin{aligned}
Z &= \int \mathcal{D}\phi^M \mathrm{e}^{\frac{i}{\hbar} S^M[\phi^M]} \\
&\downarrow \quad \hbar = 1, \quad \tau \to -it \qquad \text{imaginary time(euclidean space)!} \\
&= \int \mathcal{D}\phi \mathrm{e}^{-S[\phi]}
\end{aligned}
$$

where $\mathcal{D}$ is an integration of all possible paths in space.
An observable O becomes,

$$
\langle O \rangle = \frac{1}{Z} \int \mathcal{D}\phi O[\phi] \mathrm{e}^{-S[\phi]}
$$

with action given in terms of spacetime integral of the Lagrangian $\mathcal{L}$

$$
S = \int \mathrm{d}^4 x \mathcal{L}
$$

- We go to imaginary time in order to avoid oscillations due to the complex phase.
- We must also change S so it is in Euclidean space.
- Then, the expectation value given in terms to all possible paths with Z as a weight.

Path integrals

Given a field ϕ^M in Minkowski space, the *partition function* Z is given by

$$
\begin{aligned}
Z &= \int \mathcal{D}\phi^M \mathrm{e}^{\frac{i}{\hbar} S^M[\phi^M]} \\
&\downarrow \quad \hbar = 1, \quad \tau \to -it \qquad \text{imaginary time(euclidean space)!} \\
&= \int \mathcal{D}\phi \mathrm{e}^{-S[\phi]}
\end{aligned}
$$

where $\mathcal{D}$ is an integration of all possible paths in space.
An observable O becomes,

$$\langle O \rangle = \frac{1}{Z} \int \mathcal{D}\phi O[\phi] \mathrm{e}^{-S[\phi]}$$

with action given in terms of spacetime integral of the Lagrangian $\mathcal{L}$

$$S = \int \mathrm{d}^4 x \mathcal{L}$$

Difficult to calculate the all possible paths $\rightarrow$ discretize spacetime

- We go to imaginary time in order to avoid oscillations due to the complex phase.
- We must also change S so it is in Euclidean space.
- Then, the expectation value given in terms to all possible paths with Z as a weight.
- It is difficult to calculate all of the possible paths, so instead we discretize spacetime with the field value at every spacetime point instead.

Path integrals

Given a field ϕ^M in Minkowski space, the *partition function* Z is given by

$$
\begin{aligned}
Z &= \int \mathcal{D}\phi^M \mathrm{e}^{\frac{i}{\hbar} S^M[\phi^M]} \\
&\downarrow \quad \hbar = 1, \quad \tau \to -it \qquad \text{imaginary time(euclidean space)!} \\
&= \int \mathcal{D}\phi \mathrm{e}^{-S[\phi]}
\end{aligned}
$$

where $\mathcal{D}$ is an integration of all possible paths in space.
An observable O becomes,

$$\langle O \rangle = \frac{1}{Z} \int \mathcal{D}\phi O[\phi] \mathrm{e}^{-S[\phi]}$$

with action given in terms of spacetime integral of the Lagrangian $\mathcal{L}$

$$S = \int \mathrm{d}^4 x \mathcal{L}$$

Difficult to calculate the all possible paths $\to$ discretize spacetime

- We go to imaginary time in order to avoid oscillations due to the complex phase.
- We must also change S so it is in Euclidean space.
- Then, the expectation value given in terms to all possible paths with Z as a weight.
- It is difficult to calculate all of the possible paths, so instead we discretize spacetime with the field value at every spacetime point instead.

Discretizing the path integral

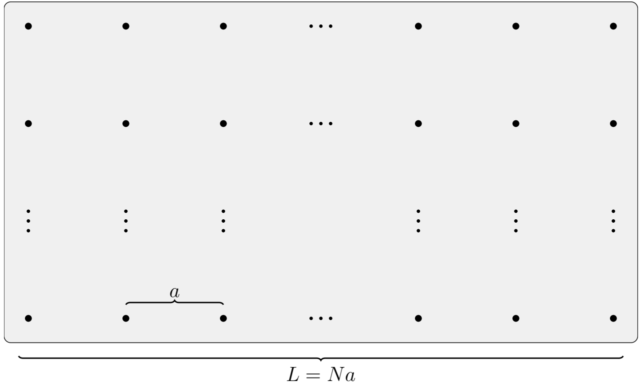

Discretizing the path integral

Path integral integration measure becomes

$$\int \mathcal{D}\phi = \prod_{x_\mu} \int \mathrm{d}\phi_{x_\mu}$$

- We now have a integral over the field at every spacetime point.

Discretizing the path integral

Path integral integration measure becomes

$$\int \mathcal{D}\phi = \prod_{x_\mu} \int \mathrm{d}\phi_{x_\mu}$$

We integrate over each spacetime point.

- We now have a integral over the field at every spacetime point.

Discretizing the path integral

Path integral integration measure becomes

$$\int \mathcal{D}\phi = \prod_{x_\mu} \int \mathrm{d}\phi_{x_\mu}$$

We integrate over each spacetime point.
$32 \times 32 \times 32 \times 32 = 2^{20} \to n^{2^{20}}$ integration points.

- We now have a integral over the field at every spacetime point.
- This poses another challenge, namely that we quickly have a large number of integrals. Say for a 32^4 lattice, we will have $n^{2^{20}}$ integration points using conventional integration methods, i.e. the trapezoidal method.

Discretizing the path integral

Path integral integration measure becomes

$$\int \mathcal{D}\phi = \prod_{x_\mu} \int \mathrm{d}\phi_{x_\mu}$$

We integrate over each spacetime point.
$32 \times 32 \times 32 \times 32 = 2^{20} \rightarrow n^{2^{20}}$ integration points.
A **statistical approach** using importance sampling is needed.

- We now have a integral over the field at every spacetime point.
- This poses another challenge, namely that we quickly have a large number of integrals. Say for a 32^4 lattice, we will have $n^{2^{20}}$ integration points using conventional integration methods, i.e. the trapezoidal method.
- This require us to use statistical methods with some sort of importance sampling.

Discretizing the path integral

Path integral integration measure becomes

$$\int \mathcal{D}\phi = \prod_{x_\mu} \int \mathrm{d}\phi_{x_\mu}$$

We integrate over each spacetime point.
$32 \times 32 \times 32 \times 32 = 2^{20} \to n^{2^{20}}$ integration points.
A **statistical approach** using importance sampling is needed.
An expectation value becomes

$$\langle O \rangle = \frac{1}{N_{\text{cfg}}} \sum_{i=1}^{N_{\text{cfg}}} O[\phi_i] + \mathcal{O}\left(\frac{1}{\sqrt{N_{\text{cfg}}}}\right)$$

- We now have a integral over the field at every spacetime point.
- This poses another challenge, namely that we quickly have a large number of integrals. Say for a 32^4 lattice, we will have $n^{2^{20}}$ integration points using conventional integration methods, i.e. the trapezoidal method.
- This require us to use statistical methods with some sort of importance sampling.
- Since we now are using a statistical method, the challenge is now to generate configurations of the spacetime that lie in the vicinity of the action minimum. The expectation value then becomes the average of such configurations, and the error of these scales with $1/\sqrt{N_{\text{cfg}}}$.

Discretizing the path integral

Path integral integration measure becomes

$$\int \mathcal{D}\phi = \prod_{x_\mu} \int \mathrm{d}\phi_{x_\mu}$$

We integrate over each spacetime point.
$32 \times 32 \times 32 \times 32 = 2^{20} \rightarrow n^{2^{20}}$ integration points.
A **statistical approach** using importance sampling is needed.
An expectation value becomes

$$\langle O \rangle = \frac{1}{N_{\mathrm{cfg}}} \sum_{i=1}^{N_{\mathrm{cfg}}} O[\phi_i] + \mathcal{O}\left(\frac{1}{\sqrt{N_{\mathrm{cfg}}}}\right)$$

- We now have a integral over the field at every spacetime point.
- This poses another challenge, namely that we quickly have a large number of integrals. Say for a 32^4 lattice, we will have $n^{2^{20}}$ integration points using conventional integration methods, i.e. the trapezoidal method.
- This require us to use statistical methods with some sort of importance sampling.
- Since we now are using a statistical method, the challenge is now to generate configurations of the spacetime that lie in the vicinity of the action minimum. The expectation value then becomes the average of such configurations, and the error of these scales with $1/\sqrt{N_{\mathrm{cfg}}}$.

QCD on the lattice

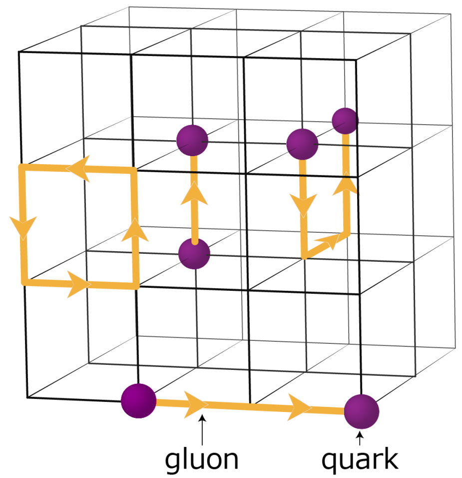

http://www.jicfus.jp/en/wp-content/uploads/2012/12/LatticeQCD.png

- The lattice is a cube in 4D.
- Quarks at lattice, gluons in-between (**links**).
- Maintains the $\mathrm{SU}(3)$ symmetry by introducing links.
- Closed loops are gauge invariant.
- Smallest possible object: the plaquette.
- Paths of links with fermions as end points are gauge invariant.
- However, from now on we will ignore any fermions.

From QCD to pure $\mathrm{SU}(3)$ Yang-Mills

We exclude fermions to only look at the gauge fields,

$$S_G = \frac{1}{2}\int \mathrm{d}^4 x \mathrm{tr}\left(F_{\mu\nu}\right)^2$$

Links

- *Links* $U_\mu(n)$ tell us how the gauge field at lattice location n changes in a given direction $\hat{\mu}$

Links

- *Links* $U_\mu(n)$ tell us how the gauge field at lattice location n changes in a given direction $\hat{\mu}$
- Four links at every lattice size(one for each Lorentz index). Opposite direction given by its inverse.

Links

- *Links* $U_\mu(n)$ tell us how the gauge field at lattice location n changes in a given direction $\hat{\mu}$
- Four links at every lattice size(one for each Lorentz index). Opposite direction given by its inverse.
- Links are complex 3×3 matrices of the group $\mathrm{SU}(3)$ with properties of,

Links

- *Links* $U_\mu(n)$ tell us how the gauge field at lattice location n changes in a given direction $\hat{\mu}$
- Four links at every lattice size(one for each Lorentz index). Opposite direction given by its inverse.
- Links are complex 3×3 matrices of the group $\mathrm{SU}(3)$ with properties of,

$$U_\mu^\dagger(x) = U_\mu^{-1}(x), \qquad \det\left(U_\mu(x)\right) = 1.$$

Links

- *Links* $U_\mu(n)$ tell us how the gauge field at lattice location n changes in a given direction $\hat{\mu}$
- Four links at every lattice size(one for each Lorentz index). Opposite direction given by its inverse.
- Links are complex 3×3 matrices of the group $\mathrm{SU}(3)$ with properties of,

$$U_\mu^\dagger(x) = U_\mu^{-1}(x), \qquad \det\left(U_\mu(x)\right) = 1.$$

From this we can build a lattice action,

$$S_G[U] = \frac{\beta}{3} \sum_{n\in\Lambda} \sum_{\mu<\nu} \mathrm{Re}\,\mathrm{tr}\left[1 - U_\mu(n)\, U_\nu(n+\hat{\mu})\, U_\mu(n+\hat{\nu})^\dagger\, U_\nu(n)^\dagger\right],$$

with $\beta = 6/g_S^2$

Notice that in this expression we have that the four links that forms a *plaqeutte*, which is the smallest possible gauge invariant object, are dependent on the neighboring object at $\hat{\mu}$ and $\hat{\nu}$.

Links

- *Links* $U_\mu(n)$ tell us how the gauge field at lattice location n changes in a given direction $\hat{\mu}$
- Four links at every lattice size(one for each Lorentz index). Opposite direction given by its inverse.
- Links are complex 3×3 matrices of the group $\mathrm{SU}(3)$ with properties of,

$$U_\mu^\dagger(x) = U_\mu^{-1}(x), \qquad \det\left(U_\mu(x)\right) = 1.$$

From this we can build a lattice action,

$$S_G[U] = \frac{\beta}{3} \sum_{n\in\Lambda} \sum_{\mu<\nu} \mathrm{Re}\,\mathrm{tr}\left[1 - U_\mu(n) U_\nu(n+\hat{\mu}) U_\mu(n+\hat{\nu})^\dagger U_\nu(n)^\dagger\right],$$

with $\beta = 6/g_S^2$

Notice that in this expression we have that the four links that forms a *plaqeutte*, which is the smallest possible gauge invariant object, are dependent on the neighboring object at $\hat{\mu}$ and $\hat{\nu}$.
Since we are dealing with $\mathrm{SU}(3)$ matrices, we have that we in reality are performing pure matrix algebra. Due to the size of the lattice we would like to split this calculation.

Links

- *Links* $U_\mu(n)$ tell us how the gauge field at lattice location n changes in a given direction $\hat{\mu}$
- Four links at every lattice size(one for each Lorentz index). Opposite direction given by its inverse.
- Links are complex 3×3 matrices of the group $\mathrm{SU}(3)$ with properties of,

$$U_\mu^\dagger(x) = U_\mu^{-1}(x), \qquad \det\left(U_\mu(x)\right) = 1.$$

From this we can build a lattice action,

$$S_G[U] = \frac{\beta}{3} \sum_{n \in \Lambda} \sum_{\mu < \nu} \operatorname{Re} \operatorname{tr} \left[1 - U_\mu(n) U_\nu(n+\hat{\mu}) U_\mu(n+\hat{\nu})^\dagger U_\nu(n)^\dagger \right],$$

with $\beta = 6/g_S^2$

Notice that in this expression we have that the four links that forms a *plaqeutte*, which is the smallest possible gauge invariant object, are dependent on the neighboring object at $\hat{\mu}$ and $\hat{\nu}$.
Since we are dealing with $\mathrm{SU}(3)$ matrices, we have that we in reality are performing pure matrix algebra. Due to the size of the lattice we would like to split this calculation.

Parallelization: distributing the problem

Parallelization: distributing the problem

Number of points in a lattice:

$$\underbrace{N^3}_{\text{Spatial}} \times \underbrace{N_T}_{\text{Temporal}} \times \underbrace{4}_{\text{Links}} \times \underbrace{9}_{\mathrm{SU}(3)\text{ matrix}} \times \underbrace{2}_{\mathbb{C}\text{-numbers}} = 72N^3N_T,$$

Parallelization: distributing the problem

Number of points in a lattice:

$$\underbrace{N^3}_{\text{Spatial}} \times \underbrace{N_T}_{\text{Temporal}} \times \underbrace{4}_{\text{Links}} \times \underbrace{9}_{\mathrm{SU}(3)\text{ matrix}} \times \underbrace{2}_{\mathbb{C}\text{-numbers}} = 72N^3N_T,$$

Too large to solve on any single computer.

Large number of d.o.f.'s → we want to split the calculation.

Parallelization: distributing the problem

Number of points in a lattice:

$$\underbrace{N^3}_{\text{Spatial}} \times \underbrace{N_T}_{\text{Temporal}} \times \underbrace{4}_{\text{Links}} \times \underbrace{9}_{\mathrm{SU}(3)\text{ matrix}} \times \underbrace{2}_{\mathbb{C}\text{-numbers}} = 72 N^3 N_T,$$

Too large to solve on any single computer.

Large number of d.o.f.'s $\rightarrow$ we want to split the calculation.

Parallelization: splitting the hypercube

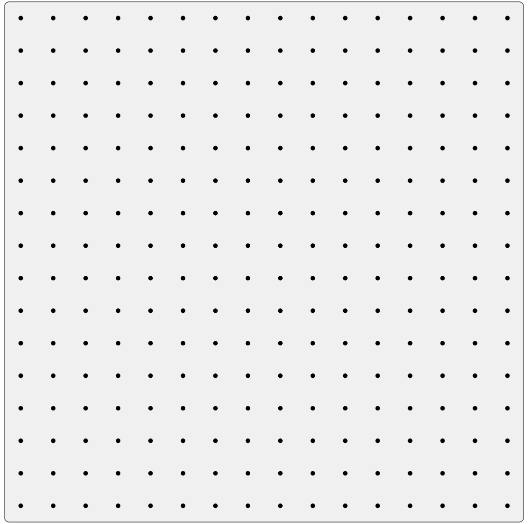

Parallelization: splitting the hypercube

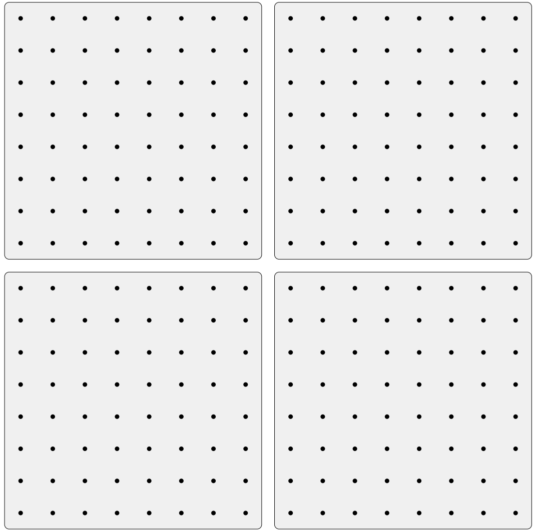

Parallelization: shifts

We need a message passing interface for communication(MPI).

Parallelization: shifts

We need a message passing interface for communication(MPI).
Implemented *shifts* for sharing data.

Parallelization: shifts

We need a message passing interface for communication(MPI).
Implemented *shifts* for sharing data.

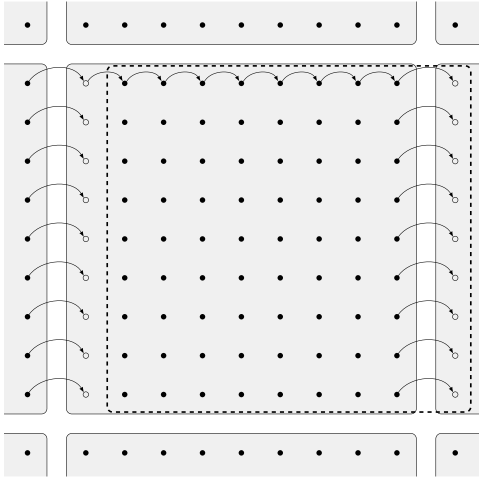

So far, we have ...

- a procedure for calculating the action using links.

- We calculate the action using links.

So far, we have ...

- a procedure for calculating the action using links.
- a statistical Monte Carlo method for solving the path integral.

- We calculate the action using links.
- We will use the Metropolis Monte Carlo method for solving the path integral and generating configurations.

So far, we have ...

- a procedure for calculating the action using links.
- a statistical Monte Carlo method for solving the path integral.
- We have a method for parallelization for handling the computations.

- We calculate the action using links.
- We will use the Metropolis Monte Carlo method for solving the path integral and generating configurations.
- We have a method for handling the computations.

So far, we have ...

- a procedure for calculating the action using links.
- a statistical Monte Carlo method for solving the path integral.
- We have a method for parallelization for handling the computations.

However, some observable are problematic...

- We calculate the action using links.
- We will use the Metropolis Monte Carlo method for solving the path integral and generating configurations.
- We have a method for handling the computations.
- However, some observables are problematic, and we need to apply some method of renormalization in order to retrieve sensible results..

So far, we have ...

- a procedure for calculating the action using links.
- a statistical Monte Carlo method for solving the path integral.
- We have a method for parallelization for handling the computations.

However, some observable are problematic...

- We calculate the action using links.

Gradient flow

$$\partial_{t_f} B_\mu(x, t_f) = D_\nu G_{\nu\mu}(x, t_f)$$
$$B_\mu(x, t_f)\big|_{t_f=0} = A_\mu(x)$$

- Solves this by integrating along t_f called *flow time* [1]

[1] Lüscher [2010]

Gradient flow

$$\partial_{t_f} B_\mu(x, t_f) = D_\nu G_{\nu\mu}(x, t_f)$$
$$B_\mu(x, t_f)\big|_{t_f=0} = A_\mu(x)$$

- Solves this by integrating along t_f called *flow time* [1]
- $B_\mu(x, t_f)$ is the gauge field $A_\mu(x)$ at a flow time t_f.

[1] Lüscher [2010]

Gradient flow

$$\partial_{t_f} B_\mu(x, t_f) = D_\nu G_{\nu\mu}(x, t_f)$$
$$B_\mu(x, t_f)\big|_{t_f=0} = A_\mu(x)$$

- Solves this by integrating along t_f called *flow time* [1]
- $B_\mu(x, t_f)$ is the gauge field $A_\mu(x)$ at a flow time t_f.
- $D_\nu = \partial_\nu + [B_\mu(x, t_f), \cdot]$

[1] Lüscher [2010]

Gradient flow

$$\partial_{t_f} B_\mu(x, t_f) = D_\nu G_{\nu\mu}(x, t_f)$$
$$B_\mu(x, t_f)\big|_{t_f=0} = A_\mu(x)$$

- Solves this by integrating along t_f called *flow time* [1]
- $B_\mu(x, t_f)$ is the gauge field $A_\mu(x)$ at a flow time t_f.
- $D_\nu = \partial_\nu + [B_\mu(x, t_f), \cdot]$
- Field strength tensor:
  $G_{\mu\nu}(x, t_f) = \partial_\mu B_\nu(x, t_f) - \partial_\nu B_\mu(x, t_f) - i[B_\mu(x, t_f), B_\nu(x, t_f)]$

[1] Lüscher [2010]

Gradient flow

$$\partial_{t_f} B_\mu(x, t_f) = D_\nu G_{\nu\mu}(x, t_f)$$
$$B_\mu(x, t_f)\big|_{t_f=0} = A_\mu(x)$$

- Solves this by integrating along t_f called *flow time* [1]
- $B_\mu(x, t_f)$ is the gauge field $A_\mu(x)$ at a flow time t_f.
- $D_\nu = \partial_\nu + [B_\mu(x, t_f), \cdot]$
- Field strength tensor:
  $G_{\mu\nu}(x, t_f) = \partial_\mu B_\nu(x, t_f) - \partial_\nu B_\mu(x, t_f) - i[B_\mu(x, t_f), B_\nu(x, t_f)]$

An analogy: the diffusion equation:

$$\frac{\partial}{\partial t_f} B_\mu(x, t_f) \approx \partial_x^2 B_\mu(x, t_f)$$

[1] Lüscher [2010]

Gradient flow II

- The gauge field at $t_f > 0$ is a **smooth, renormalized field**.

Gradient flow II

- The gauge field at $t_f > 0$ is a **smooth, renormalized field**.
- Allows us to measure certain quantities such as the **topological charge**, Q

Gradient flow II

- The gauge field at $t_f > 0$ is a **smooth, renormalized field**.
- Allows us to measure certain quantities such as the **topological charge**, Q

Solve on the lattice using the symplectic, structure preserving Runge-Kutta 3 solver[2]

Gradient flow III: topological charge

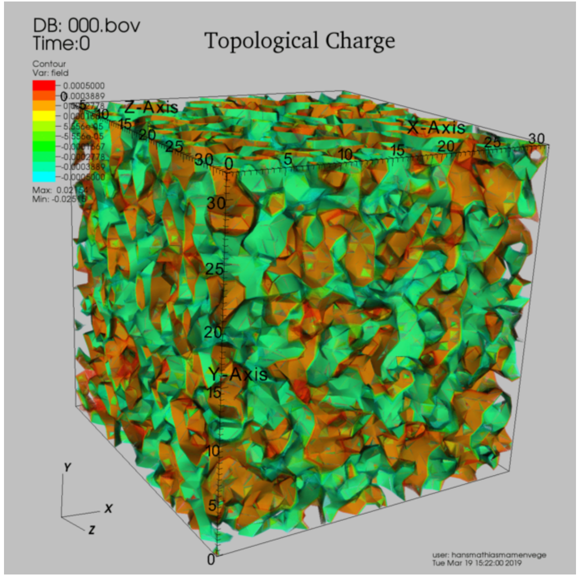

Evolution of topological charge Q in flow time.

Results

Ensembles

Points in lattice given by $N^3 \times N_T$.

Ensemble	$\beta = 6/g_S^2$	N	N_T	N_{cfg}	a [fm]	Config. size[GB]
A	6.0	24	48	1000	$0.0931(4)$	0.356
B	6.1	28	56	1000	$0.0791(3)$	0.659
C	6.2	32	64	2000	$0.0679(3)$	1.125
D_1	6.45	32	32	1000	$0.0478(3)$	0.563
D_2	6.45	48	96	250	$0.0478(3)$	5.695

- I implemented the methods discussed under a code I call GLAC, and will now present some of the results I generated using this code.
- The main ensembles made for this thesis.
- Notice that the size of a lattice is 16 times larger when doubling the dimensions.
- Every configuration was flown with $N_{\text{flow}} = 1000$ flow steps.
- Since there is are so few data configurations, resampling techniques such as bootstrapping were implemented.

Topological charge

- QCC vacua(i.e. gauge fields) can be classified by their topological properties.

Topological charge

- QCC vacua(i.e. gauge fields) can be classified by their topological properties.
- In this vacua, **Instantons** are local minimums of the Yang-Mills action in Euclidean space.

- **Instantons** are local minimums to the Yang-Mills action in Euclidean space.

Topological charge

- QCC vacua(i.e. gauge fields) can be classified by their topological properties.
- In this vacua, **Instantons** are local minimums of the Yang-Mills action in Euclidean space.
- **Topological charge** Q can be viewed as a “measure” of instantons.

- **Instantons** are local minimums to the Yang-Mills action in Euclidean space.
- Instantons are significant in LQCD because of *critical slowdown* which we will return to later.

Topological charge

- QCC vacua(i.e. gauge fields) can be classified by their topological properties.
- In this vacua, **Instantons** are local minimums of the Yang-Mills action in Euclidean space.
- **Topological charge** Q can be viewed as a “measure” of instantons.

$$Q = a^4 \sum_{n\in\Lambda} q(n),$$

with the charge density given by

$$q(n) = \frac{1}{32\pi^2}\epsilon_{\mu\nu\rho\sigma}\mathrm{tr}\left[F_{\mu\nu}(n)F_{\rho\sigma}(n)\right].$$

- **Instantons** are local minimums to the Yang-Mills action in Euclidean space.
- Instantons are significant in LQCD because of *critical slowdown* which we will return to later.
- The charge is a **sum over the local charge** at every point in the gauge field.
- Can in a very crude manner be viewed as the “curl” of the gauge fields due to the Levi-Civita tensor.

Topological charge

- QCC vacua(i.e. gauge fields) can be classified by their topological properties.
- In this vacua, **Instantons** are local minimums of the Yang-Mills action in Euclidean space.
- **Topological charge** Q can be viewed as a "measure" of instantons.

$$Q = a^4 \sum_{n \in \Lambda} q(n),$$

with the charge density given by

$$q(n) = \frac{1}{32\pi^2} \epsilon_{\mu\nu\rho\sigma} \mathrm{tr}\left[F_{\mu\nu}(n) F_{\rho\sigma}(n)\right].$$

Equally probably to have negative charge as positive,

$$\langle Q \rangle = 0$$

- **Instantons** are local minimums to the Yang-Mills action in Euclidean space.
- Instantons are significant in LQCD because of *critical slowdown* which we will return to later.
- The charge is a **sum over the local charge** at every point in the gauge field.
- Can in a very crude manner be viewed as the "curl" of the gauge fields due to the Levi-Civita tensor.
- The **expectation value** of Q **is zero** due to it being **parity odd**.

Topological charge

- QCC vacua(i.e. gauge fields) can be classified by their topological properties.
- In this vacua, **Instantons** are local minimums of the Yang-Mills action in Euclidean space.
- **Topological charge** Q can be viewed as a "measure" of instantons.

$$Q = a^4 \sum_{n \in \Lambda} q(n),$$

with the charge density given by

$$q(n) = \frac{1}{32\pi^2} \epsilon_{\mu\nu\rho\sigma} \mathrm{tr}\left[F_{\mu\nu}(n) F_{\rho\sigma}(n)\right].$$

Equally probably to have negative charge as positive,

$$\langle Q \rangle = 0$$

- **Instantons** are local minimums to the Yang-Mills action in Euclidean space.
- Instantons are significant in LQCD because of *critical slowdown* which we will return to later.
- The charge is a **sum over the local charge** at every point in the gauge field.
- Can in a very crude manner be viewed as the "curl" of the gauge fields due to the Levi-Civita tensor.
- The **expectation value** of Q **is zero** due to it being **parity odd**.

Topological charge distribution

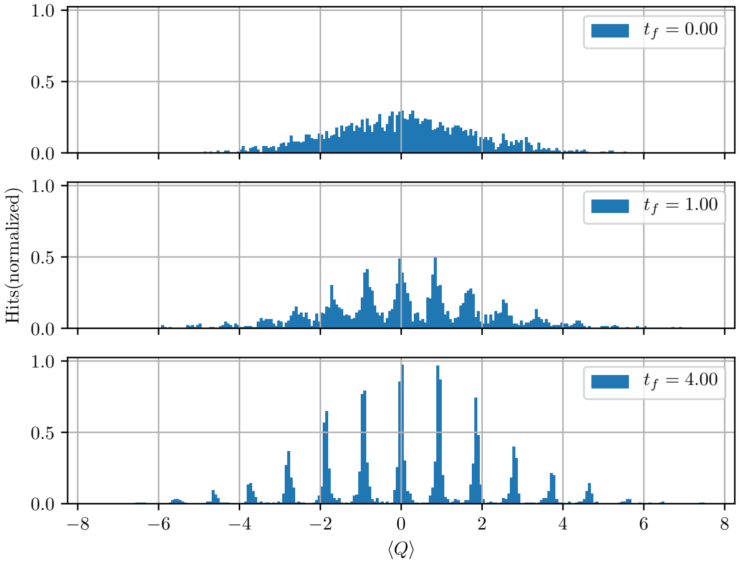

Histograms for the Q for ensemble G with a lattice of size $N^3 \times N_T = 16^3 \times 32$ with $\beta = 6.1$, taken at different flow times $t_f/a^2 = 0.0, 1.0, 4.0$ fm.

Topological charge

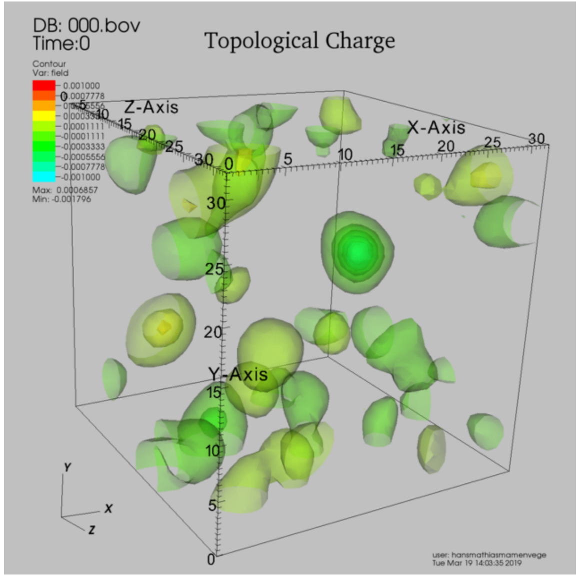

Topological charge for our main ensembles

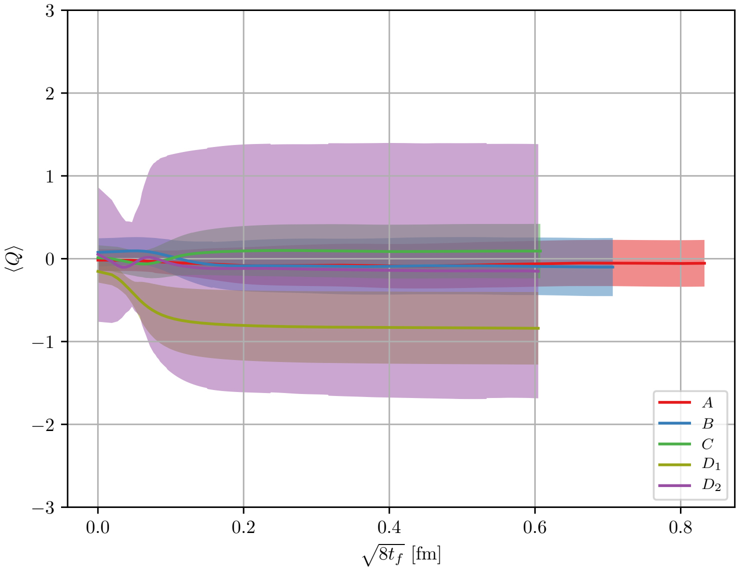

Autocorrelations

- Why is the charge not centered around zero for certain ensembles?

Autocorrelations

- Why is the charge not centered around zero for certain ensembles?
- Let us look at the **autocorrelation** - the measure for correlations between gauge configurations in Monte Carlo time.

Autocorrelations

- Why is the charge not centered around zero for certain ensembles?
- Let us look at the **autocorrelation** - the measure for correlations between gauge configurations in Monte Carlo time.
- The autocorrelation is given as $\Gamma(t) = \langle (a_i - a)(a_{i+1} - a) \rangle$ and $\tau_{\text{int}} = \frac{1}{2} + \sum_{t=1}^{\infty} \frac{\Gamma(t)}{\Gamma(0)}$.

Autocorrelations

- Why is the charge not centered around zero for certain ensembles?
- Let us look at the **autocorrelation** - the measure for correlations between gauge configurations in Monte Carlo time.
- The autocorrelation is given as $\Gamma(t) = \langle (a_i - a)(a_{i+1} - a) \rangle$ and $\tau_{\mathrm{int}} = \frac{1}{2} + \sum_{t=1}^{\infty} \frac{\Gamma(t)}{\Gamma(0)}$.
- **Zero autocorrelation** corresponds to $\tau_{\mathrm{int}} = 0.5$

Autocorrelations

- Why is the charge not centered around zero for certain ensembles?
- Let us look at the **autocorrelation** - the measure for correlations between gauge configurations in Monte Carlo time.
- The autocorrelation is given as $\Gamma(t) = \langle (a_i - a)(a_{i+1} - a) \rangle$ and $\tau_{\text{int}} = \frac{1}{2} + \sum_{t=1}^{\infty} \frac{\Gamma(t)}{\Gamma(0)}$.
- **Zero autocorrelation** corresponds to $\tau_{\text{int}} = 0.5$

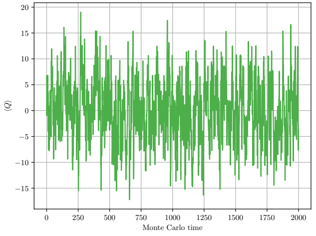

Ensemble C, $32^3 \times 64$, $\beta = 6.2$

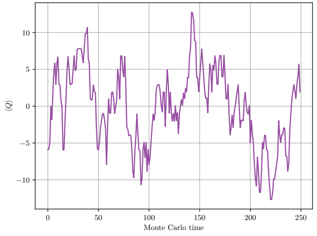

Ensemble D_2, $48^3 \times 96$, $\beta = 6.45$

Autocorrelation in the energy

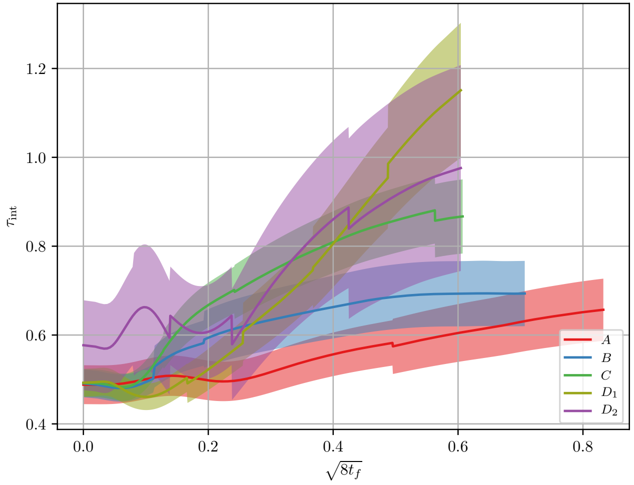

The autocorrelation of the energy. A value of $\tau_{\mathrm{int}} = 0.5$ indicates that we have zero autocorrelation.

Topological charge autocorrelation

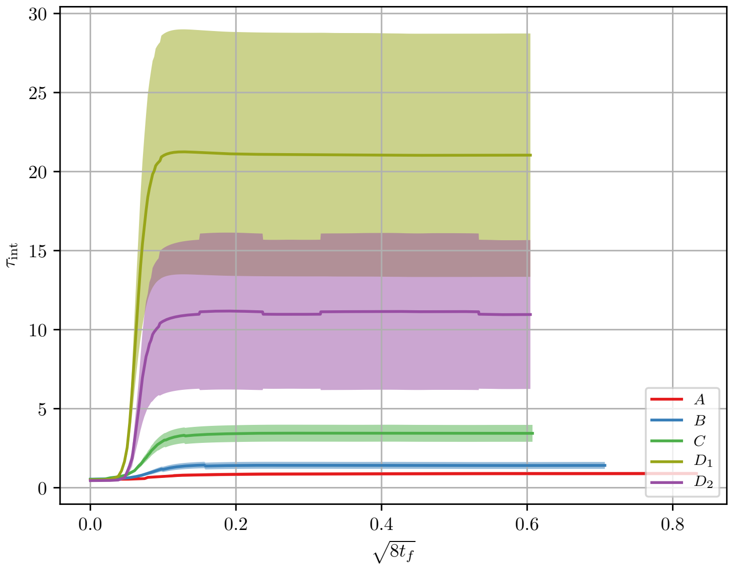

- The integrated autocorrelation $\tau_{\rm int}$ for topological charge for the five main ensembles.

Critical slowdown

Critical slowdown is the phenomena where we as the lattice spacing a *decreases* the required energy to tunnel from one state to another *increase*.

Critical slowdown

Critical slowdown is the phenomena where we as the lattice spacing a *decreases* the required energy to tunnel from one state to another *increase*.
$\rightarrow$ many more lattice updates are required in order to have independent gauge configurations.

- That is, going from one instanton sector to another requires many more updates and becomes an inherent problem in all LQCD calculations.

Critical slowdown

Critical slowdown is the phenomena where we as the lattice spacing a *decreases* the required energy to tunnel from one state to another *increase*.
$\rightarrow$ many more lattice updates are required in order to have independent gauge configurations.

- That is, going from one instanton sector to another requires many more updates and becomes an inherent problem in all LQCD calculations.
- In the continuum it would require an **infinite amount of energy** to go from **one instanton sector to another**. Thus as we a **approaches the continuum**, the amount of **effort**(number of updates ect.) required to generate **independent** gauge configurations **increases**.

Critical slowdown

Critical slowdown is the phenomena where we as the lattice spacing a *decreases* the required energy to tunnel from one state to another *increase*.
$\rightarrow$ many more lattice updates are required in order to have independent gauge configurations.

- That is, going from one instanton sector to another requires many more updates and becomes an inherent problem in all LQCD calculations.
- In the continuum it would require an **infinite amount of energy** to go from **one instanton sector to another**. Thus as we a **approaches the continuum**, the amount of **effort**(number of updates ect.) required to generate **independent** gauge configurations **increases**.

Topological susceptibility

The *topological susceptibility* is given by

$$\chi_{\mathrm{top}}^{1/4} = \frac{1}{V^{1/4}} \left\langle Q^2 \right\rangle^{1/4}$$

with V being the lattice volume and $\left\langle Q^2 \right\rangle$ is the second momenta of the charge.

Topological susceptibility

The *topological susceptibility* is given by

$$\chi_{\text{top}}^{1/4} = \frac{1}{V^{1/4}} \left\langle Q^2 \right\rangle^{1/4}$$

with V being the lattice volume and $\left\langle Q^2 \right\rangle$ is the second momenta of the charge.
The *Witten-Veneziano relation* is given by

$$m_{\eta'}^2 = \frac{2N_f}{f_\pi^2} \chi_{\text{top}}$$

- R.h.s. is full QCD and l.h.s is from pure gauge theory.

Topological susceptibility

The *topological susceptibility* is given by

$$\chi_{\text{top}}^{1/4} = \frac{1}{V^{1/4}} \left\langle Q^2 \right\rangle^{1/4}$$

with V being the lattice volume and $\left\langle Q^2 \right\rangle$ is the second momenta of the charge.
The *Witten-Veneziano relation* is given by

$$m_{\eta'}^2 = \frac{2N_f}{f_\pi^2} \chi_{\text{top}}$$

with

- pion decay constant $f_\pi = 0.130(5)/\sqrt{2}$ GeV.

- R.h.s. is full QCD and l.h.s is from pure gauge theory.
- We can use the Witten-Veneziano formula in order to extract an estimate for N_f using the topological susceptibility.

Topological susceptibility

The *topological susceptibility* is given by

$$\chi_{\text{top}}^{1/4} = \frac{1}{V^{1/4}} \left\langle Q^2 \right\rangle^{1/4}$$

with V being the lattice volume and $\left\langle Q^2 \right\rangle$ is the second momenta of the charge.
The *Witten-Veneziano relation* is given by

$$m_{\eta'}^2 = \frac{2N_f}{f_\pi^2} \chi_{\text{top}}$$

with

- pion decay constant $f_\pi = 0.130(5)/\sqrt{2}$ GeV.
- η' meson mass $m_{\eta'} = 0.95778(6)$ GeV.

- R.h.s. is full QCD and l.h.s is from pure gauge theory.
- We can use the Witten-Veneziano formula in order to extract an estimate for N_f using the topological susceptibility.

Topological susceptibility

The *topological susceptibility* is given by

$$\chi_{\text{top}}^{1/4} = \frac{1}{V^{1/4}} \left\langle Q^2 \right\rangle^{1/4}$$

with V being the lattice volume and $\left\langle Q^2 \right\rangle$ is the second momenta of the charge.
The *Witten-Veneziano relation* is given by

$$m_{\eta'}^2 = \frac{2N_f}{f_\pi^2} \chi_{\text{top}}$$

with

- pion decay constant $f_\pi = 0.130(5)/\sqrt{2}$ GeV.
- η' meson mass $m_{\eta'} = 0.95778(6)$ GeV.
- N_f is the number of flavors(i.e. quark species involved in η'.).

- R.h.s. is full QCD and l.h.s is from pure gauge theory.
- We can use the Witten-Veneziano formula in order to extract an estimate for N_f using the topological susceptibility.

Topological susceptibility

The *topological susceptibility* is given by

$$\chi_{\text{top}}^{1/4} = \frac{1}{V^{1/4}} \left\langle Q^2 \right\rangle^{1/4}$$

with V being the lattice volume and $\left\langle Q^2 \right\rangle$ is the second momenta of the charge.
The *Witten-Veneziano relation* is given by

$$m_{\eta'}^2 = \frac{2N_f}{f_\pi^2}\chi_{\text{top}}$$

with

- pion decay constant $f_\pi = 0.130(5)/\sqrt{2}$ GeV.
- η' meson mass $m_{\eta'} = 0.95778(6)$ GeV.
- N_f is the number of flavors(i.e. quark species involved in η'.).

We expect $N_f = 3$.

- R.h.s. is full QCD and l.h.s is from pure gauge theory.
- We can use the Witten-Veneziano formula in order to extract an estimate for N_f using the topological susceptibility.
- This can help us understand the "quality" of the ensemble, as we would expect to be around $N_f = 3$.

Topological susceptibility

The *topological susceptibility* is given by

$$\chi_{\text{top}}^{1/4} = \frac{1}{V^{1/4}} \left\langle Q^2 \right\rangle^{1/4}$$

with V being the lattice volume and $\left\langle Q^2 \right\rangle$ is the second momenta of the charge.
The *Witten-Veneziano relation* is given by

$$m_{\eta'}^2 = \frac{2N_f}{f_\pi^2} \chi_{\text{top}}$$

with

- pion decay constant $f_\pi = 0.130(5)/\sqrt{2}$ GeV.
- η' meson mass $m_{\eta'} = 0.95778(6)$ GeV.
- N_f is the number of flavors(i.e. quark species involved in η'.).

We expect $N_f = 3$.

- R.h.s. is full QCD and l.h.s is from pure gauge theory.
- We can use the Witten-Veneziano formula in order to extract an estimate for N_f using the topological susceptibility.
- This can help us understand the "quality" of the ensemble, as we would expect to be around $N_f = 3$.

Topological susceptibility

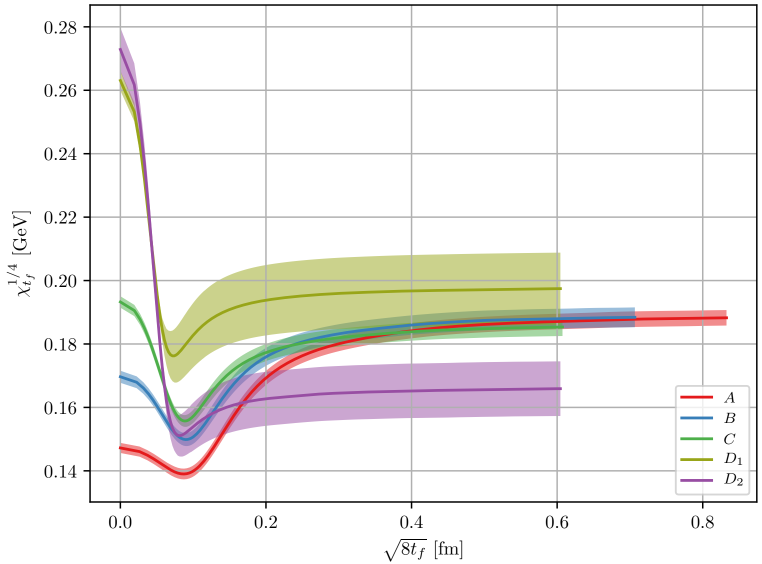

- The topological susceptibility $\chi_{t_f}^{1/4}$ of the **main ensembles**.
- We have a **UV divergence at zeroth flow time**, hence to need for gradient flow which renormalizes this quantity.
- **Bootstrapped** $N_{\rm bs} = 500$ times.
- **Corrected for autocorrelations** with $\sigma = \sqrt{2\tau_{\rm int}}\sigma_0$.

Topological susceptibility continuum extrapolation

Ensembles	$\chi_{t_f}^{1/4}$ ($\langle Q^2 \rangle$) [GeV]	N_f	χ^2/d.o.f
A, B, C, D_2	$0.179(10)$	$3.75(29)$	2.38
A, B, C, D_1	$0.186(6)$	$3.21(25)$	0.83
B, C, D_1	$0.187(24)$	$3.18(24)$	1.63
B, C, D_2	$0.166(24)$	$5.06(39)$	2.05
A, B, C	$0.184(6)$	$3.37(26)$	0.33

The fourth cumulant

$$\left\langle Q^4 \right\rangle_c = \frac{1}{V^2} \left(\left\langle Q^4 \right\rangle - 3 \left\langle Q^2 \right\rangle^2 \right).$$

From this, we can also measure the ratio R,

$$R = \frac{\left\langle Q^4 \right\rangle_c}{\frac{1}{V} \left\langle Q^2 \right\rangle} = \frac{1}{V} \frac{\left\langle Q^4 \right\rangle - 3 \left\langle Q^2 \right\rangle^2}{\left\langle Q^2 \right\rangle},$$

- Highly unstable, as we shall see.
- Will provide insight into the goodness of our ensembles.
- An R-value away from 1 will indicate that QCD cannot be described by the dilute instanton gas model.

The fourth cumulant

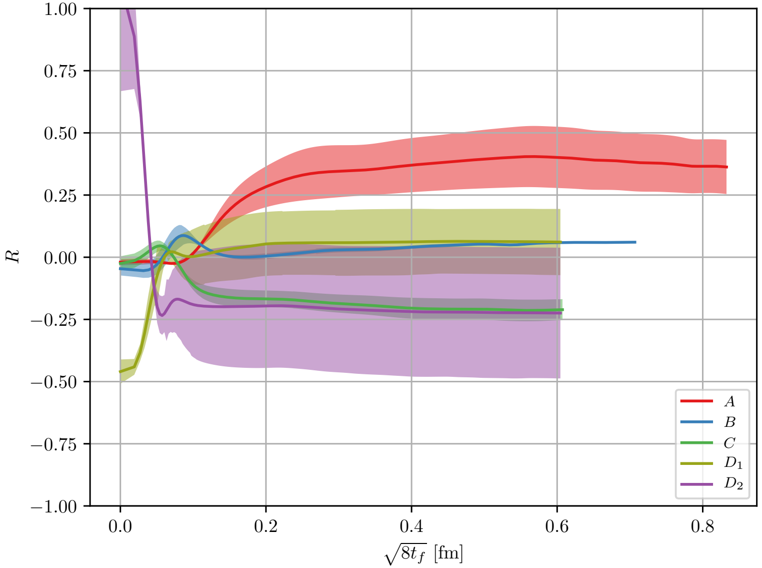

- The fourth cumulant ratio $R = \langle Q^4 \rangle_C / \langle Q^2 \rangle$.
- The results was analyzed using $N_{\mathrm{bs}} = 500$ bootstrap samples, with the error corrected for by $\sqrt{2\tau_{\mathrm{int}}}$.

The fourth cumulant at reference flow times

Ensemble	L/a	t_0/a^2	$\langle Q^2 \rangle$	$\langle Q^4 \rangle$	$\langle Q^4 \rangle_C$	R
A	2.24	3.20(3)	0.78(4)	2.13(27)	0.282(67)	0.359(65)
B	2.21	4.43(4)	0.81(5)	1.98(23)	0.036(11)	0.044(11)
C	2.17	6.01(6)	0.77(4)	1.6(2)	−0.174(40)	−0.226(64)
D_1	1.53	12.2(1)	1.00(20)	3.01(1.07)	0.03(12)	0.03(12)
D_2	2.29	12.2(1)	0.497(100)	0.64(20)	−0.103(95)	−0.21(23)

The fourth cumulant is taken at their individual reference scales seen in the third column. The data were analyzed with using a bootstrap analysis of $N_{bs} = 500$ samples, with error corrected by the integrated autocorrelation, $\sqrt{2\tau_{\mathrm{int}}}$.

Comparing fourth cumulant

We can compare with article by Cè et al. [2015]

Comparing fourth cumulant

Ensemble	β	L/a	L [fm]	a [fm]	t_0/a^2	t_0/r_0^2	N_{cfg}
F_1	5.96	16	1.632	0.102	2.7887(2)	0.1113(9)	1 440 000
B_2	6.05	14	1.218	0.087	3.7960(12)	0.1114(9)	144 000
$\tilde{D}_2$		17	1.479		3.7825(8)	0.1110(9)	
B_3	6.13	16	1.232	0.077	4.8855(15)	0.1113(10)	144 000
$\tilde{D}_3$		19	1.463		4.8722(11)	0.1110(10)	
B_4	6.21	18	1.224	0.068	6.2191(20)	0.1115(11)	144 000
$\tilde{D}_4$		21	1.428		6.1957(14)	0.1111(11)	

- Parameters of the ensembles presented by Cè et al. [2015]. The first column is the ensemble name from the article. The letter indicates the volume, while the subindex indicates the β value. Ensembles of similar letters keep approximately the same length L.

Comparing fourth cumulant

Ensemble	$\langle Q^2 \rangle_{\text{normed}}$	$\langle Q^4 \rangle_{\text{normed}}$	$\langle Q^4 \rangle_{C,\text{normed}}$	R_{normed}
F_1	$0.728(1)$	$1.608(4)$	$0.016(1)$	$0.022(1)$
B_2	$0.772(3)$	$1.873(19)$	$0.085(4)$	$0.110(5)$
$\tilde{D}_2$	$0.770(3)$	$1.817(17)$	$0.037(4)$	$0.048(5)$
B_3	$0.760(3)$	$1.805(17)$	$0.074(3)$	$0.097(4)$
$\tilde{D}_3$	$0.769(3)$	$1.801(14)$	$0.027(1)$	$0.035(1)$
B_4	$0.776(3)$	$1.874(18)$	$0.069(3)$	$0.089(4)$
$\tilde{D}_4$	$0.785(3)$	$1.891(17)$	$0.040(4)$	$0.052(5)$

- Results as presented by Cè et al. [2015], **normalized by the lattice volume**.

Comparing fourth cumulant

Article	Thesis	Ratio($\langle Q^2 \rangle$)	Ratio($\langle Q^4 \rangle$)	Ratio($\langle Q^4 \rangle_C$)	Ratio(R)
F_1	A	$1.08(6)$	$1.34(18)$	$19.03(5.81)$	$17.64(4.48)$
B_2	A	$1.02(5)$	$1.15(15)$	$3.60(1.09)$	$3.54(90)$
	B	$1.04(6)$	$1.06(11)$	$0.480(74)$	$0.46(4)$
$\tilde{D}_2$	A	$1.02(5)$	$1.19(15)$	$8.31(1.99)$	$8.15(1.56)$
	B	$1.05(6)$	$1.10(12)$	$1.1(1)$	$1.06(3)$
B_3	B	$1.06(6)$	$1.10(12)$	$0.550(86)$	$0.52(5)$
$\tilde{D}_3$	B	$1.05(6)$	$1.11(12)$	$1.51(23)$	$1.4(1)$
B_4	C	$0.99(5)$	$0.86(8)$	$-2.32(46)$	$-2.35(59)$
$\tilde{D}_4$	C	$0.98(5)$	$0.85(8)$	$-3.95(96)$	$-4.05(1.19)$

- A comparison between the results obtained in this thesis on the fourth cumulant, and by those similar in volume form Cè et al. [2015]. *Ratio* indicates that we are dividing our results by the ones in previous table.

Comparing fourth cumulant

Article	Thesis	Ratio($\langle Q^2 \rangle$)	Ratio($\langle Q^4 \rangle$)	Ratio($\langle Q^4 \rangle_C$)	Ratio(R)
F_1	A	$1.08(6)$	$1.34(18)$	$19.03(5.81)$	$17.64(4.48)$
B_2	A	$1.02(5)$	$1.15(15)$	$3.60(1.09)$	$3.54(90)$
	B	$1.04(6)$	$1.06(11)$	$0.480(74)$	$0.46(4)$
$\tilde{D}_2$	A	$1.02(5)$	$1.19(15)$	$8.31(1.99)$	$8.15(1.56)$
	B	$1.05(6)$	$1.10(12)$	$1.1(1)$	$1.06(3)$
B_3	B	$1.06(6)$	$1.10(12)$	$0.550(86)$	$0.52(5)$
$\tilde{D}_3$	B	$1.05(6)$	$1.11(12)$	$1.51(23)$	$1.4(1)$
B_4	C	$0.99(5)$	$0.86(8)$	$-2.32(46)$	$-2.35(59)$
$\tilde{D}_4$	C	$0.98(5)$	$0.85(8)$	$-3.95(96)$	$-4.05(1.19)$

- A comparison between the results obtained in this thesis on the fourth cumulant, and by those similar in volume form Cè et al. [2015]. *Ratio* indicates that we are dividing our results by the ones in previous table.

The topological charge correlator

The **topological charge correlator**

$$C(n_t) = \langle q(n_t) q(0) \rangle \,,$$

$q(0)$ is the *source* placed at a fixed Euclidean time, and $q(n_t)$ is the *sink* which is summed across all Euclidean times.

- $q(0)$ is not required to be at $n_t = 0$.

The topological charge correlator

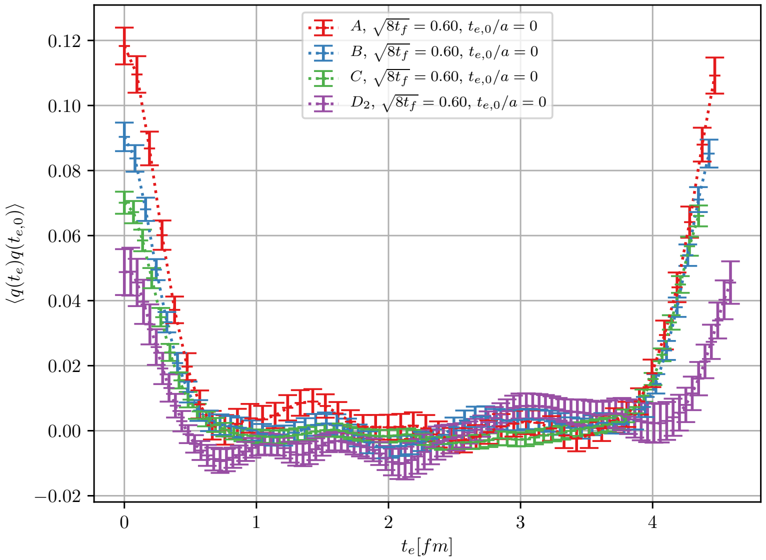

- The topological charge correlator for all of the ensembles except D_1. The x-axis contains the sink-source separation, as the source $q(0)$ is placed at $t_e = 0$ fm, and the sink $q(t_e)$ is taken at t_e.

The topological charge correlator

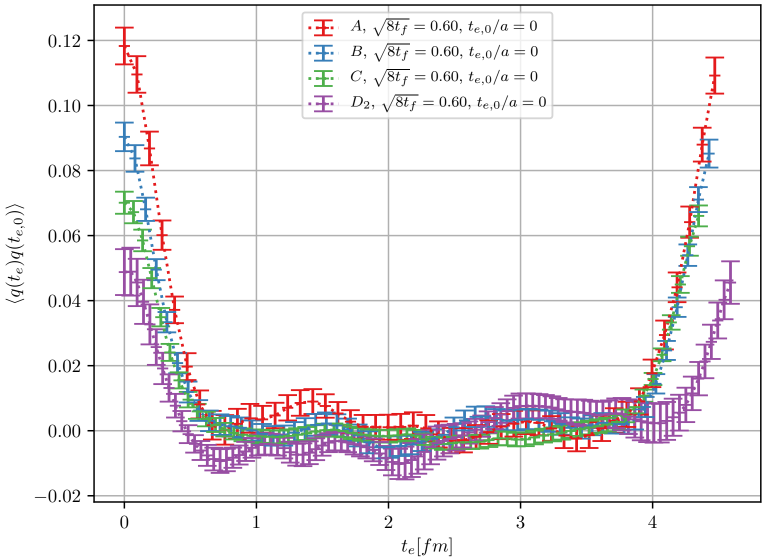

- The topological charge correlator for all of the ensembles except D_1. The x-axis contains the sink-source separation, as the source $q(0)$ is placed at $t_e = 0$ fm, and the sink $q(t_e)$ is taken at t_e.
- We since the ensembles are of different lattice sizes, we plot th D_1 separately.

The topological charge correlator

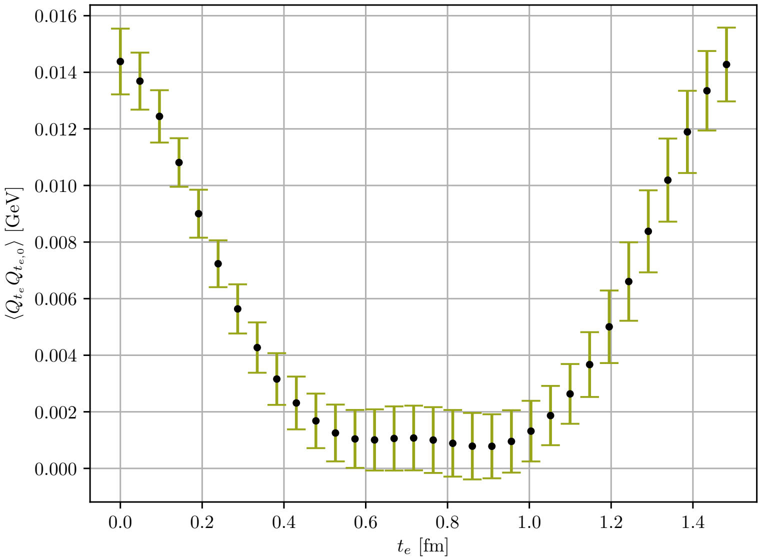

- The topological charge correlator for all of the ensembles except D_1. The x-axis contains the sink-source separation, as the source $q(0)$ is placed at $t_e = 0$ fm, and the sink $q(t_e)$ is taken at t_e.
- We since the ensembles are of different lattice sizes, we plot th D_1 separately.
- The topological charge correlator for the D_1. The source $q(0)$ is placed at $t_e = 0$ fm and the sink $q(t_e)$ is taken at t_e.

The topological charge correlator

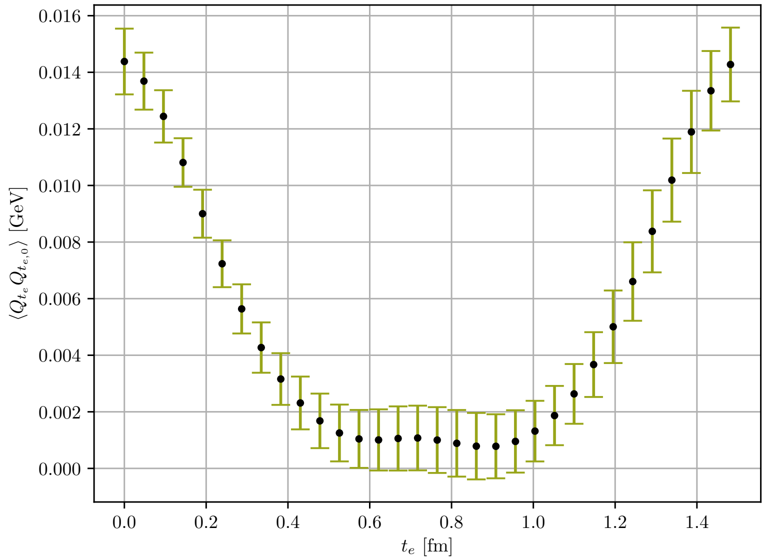

- The topological charge correlator for all of the ensembles except D_1. The x-axis contains the sink-source separation, as the source $q(0)$ is placed at $t_e = 0$ fm, and the sink $q(t_e)$ is taken at t_e.
- We since the ensembles are of different lattice sizes, we plot th D_1 separately.
- The topological charge correlator for the D_1. The source $q(0)$ is placed at $t_e = 0$ fm and the sink $q(t_e)$ is taken at t_e.
- We would expect an **exponential dampening**.

The topological charge correlator

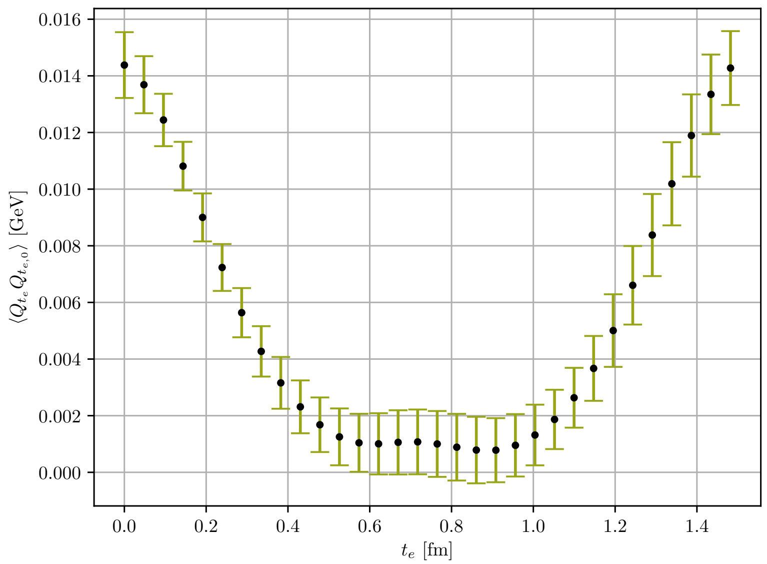

- The topological charge correlator for all of the ensembles except D_1. The x-axis contains the sink-source separation, as the source $q(0)$ is placed at $t_e = 0$ fm, and the sink $q(t_e)$ is taken at t_e.
- We since the ensembles are of different lattice sizes, we plot th D_1 separately.
- The topological charge correlator for the D_1. The source $q(0)$ is placed at $t_e = 0$ fm and the sink $q(t_e)$ is taken at t_e.
- We would expect an **exponential dampening**.

The effective glueball mass

A glueball is a bound state of gluons.

In pure Yang-Mills gauge theory, the states are stable.
We will be looking at the state involving topological charge.

The effective glueball mass

A glueball is a bound state of gluons.
The ground state in the correlator is given as

$$C(n_t) = A_0 \mathrm{e}^{-n_t E_0} + A_1 \mathrm{e}^{-n_t E_1} + \ldots$$

In pure Yang-Mills gauge theory, the states are stable.
We will be looking at the state involving topological charge.

The effective glueball mass

A glueball is a bound state of gluons.
The ground state in the correlator is given as

$$C(n_t) = A_0 \mathrm{e}^{-n_t E_0} + A_1 \mathrm{e}^{-n_t E_1} + \dots$$

which can be extracted as

$$a m_{\mathrm{eff}} = \log\left(\frac{C(n_t)}{C(n_t+1)}\right),$$

In pure Yang-Mills gauge theory, the states are stable.
We will be looking at the state involving topological charge.

The effective glueball mass

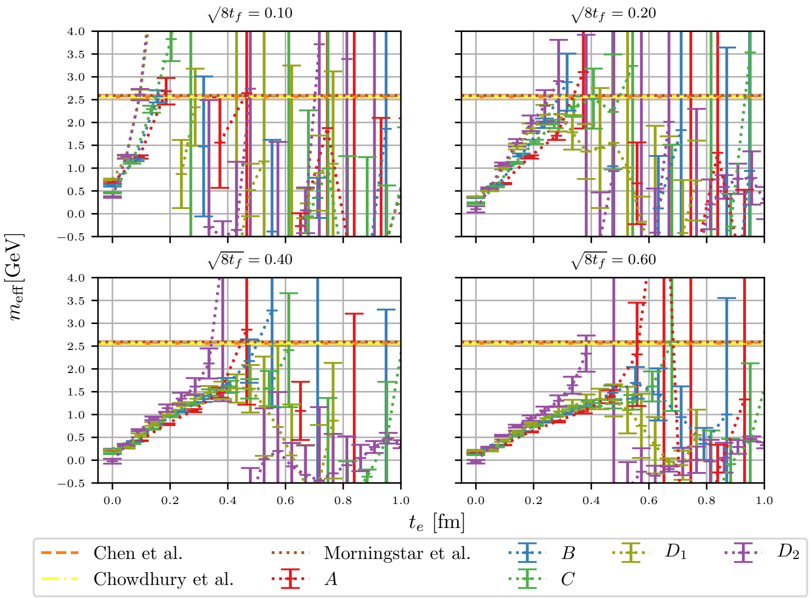

Conclusion, future developments and final thoughts

Conclusion

- Created a code capable of generating and flowing gauge configurations.

- Checked scaling and parameter optimization.

Conclusion

- Created a code capable of generating and flowing gauge configurations.
  - Verified to match other code bases down to machine precision.

- Checked scaling and parameter optimization.
- Same results as Chroma down to machine precision.

Conclusion

- Created a code capable of generating and flowing gauge configurations.
  - Verified to match other code bases down to machine precision.
- t_0 and w_0 match other papers, e.g. Lüscher [2010] and Cè et al. [2015].

- Checked scaling and parameter optimization.
- Same results as Chroma down to machine precision.
- t_0 and w_0 match other papers.

Conclusion

- Created a code capable of generating and flowing gauge configurations.
  - Verified to match other code bases down to machine precision.
- t_0 and w_0 match other papers, e.g. Lüscher [2010] and Cè et al. [2015].
- $\langle Q \rangle \neq 0$ for some ensembles.

- Checked scaling and parameter optimization.
- Same results as Chroma down to machine precision.
- t_0 and w_0 match other papers.
- $\langle Q \rangle$

Conclusion

- Created a code capable of generating and flowing gauge configurations.
  - Verified to match other code bases down to machine precision.
- t_0 and w_0 match other papers, e.g. Lüscher [2010] and Cè et al. [2015].
- $\langle Q \rangle \neq 0$ for some ensembles.
- The topological susceptibility $\left\langle \chi_f^{1/4} \right\rangle$ and N_f

- Checked scaling and parameter optimization.
- Same results as Chroma down to machine precision.
- t_0 and w_0 match other papers.
- $\langle Q \rangle$
- $\chi_f^{1/4}$. Matches well with other papers

Conclusion

- Created a code capable of generating and flowing gauge configurations.
  - Verified to match other code bases down to machine precision.
- t_0 and w_0 match other papers, e.g. Lüscher [2010] and Cè et al. [2015].
- $\langle Q \rangle \neq 0$ for some ensembles.
- The topological susceptibility $\left\langle \chi_f^{1/4} \right\rangle$ and N_f
- $\left\langle Q^4 \right\rangle_C$ and R. Sensitive quantities - need large statistics.

- Checked scaling and parameter optimization.
- Same results as Chroma down to machine precision.
- t_0 and w_0 match other papers.
- $\langle Q \rangle$
- $\chi_f^{1/4}$. Matches well with other papers
- $\left\langle Q^4 \right\rangle_C$ and R. Sensitive quantity, matches well of first and second moment.

Conclusion

- Created a code capable of generating and flowing gauge configurations.
  - Verified to match other code bases down to machine precision.
- t_0 and w_0 match other papers, e.g. Lüscher [2010] and Cè et al. [2015].
- $\langle Q \rangle \neq 0$ for some ensembles.
- The topological susceptibility $\left\langle \chi_f^{1/4} \right\rangle$ and N_f
- $\left\langle Q^4 \right\rangle_C$ and R. Sensitive quantities - need large statistics.
- Topological charge correlator $\langle q(n_t) q(0) \rangle$ and glueball mass.

- Checked scaling and parameter optimization.
- Same results as Chroma down to machine precision.
- t_0 and w_0 match other papers.
- $\langle Q \rangle$
- $\chi_f^{1/4}$. Matches well with other papers
- $\left\langle Q^4 \right\rangle_C$ and R. Sensitive quantity, matches well of first and second moment.
- Topological charge correlator $\langle q(n_t) q(0) \rangle$ and glueball mass.

Conclusion

- Created a code capable of generating and flowing gauge configurations.
  - Verified to match other code bases down to machine precision.
- t_0 and w_0 match other papers, e.g. Lüscher [2010] and Cè et al. [2015].
- $\langle Q \rangle \neq 0$ for some ensembles.
- The topological susceptibility $\left\langle \chi_f^{1/4} \right\rangle$ and N_f
- $\left\langle Q^4 \right\rangle_C$ and R. Sensitive quantities - need large statistics.
- Topological charge correlator $\langle q(n_t) q(0) \rangle$ and glueball mass.
- Statistics, autocorrelation and critical slowdown.

- Checked scaling and parameter optimization.
- Same results as Chroma down to machine precision.
- t_0 and w_0 match other papers.
- $\langle Q \rangle$
- $\chi_f^{1/4}$. Matches well with other papers
- $\left\langle Q^4 \right\rangle_C$ and R. Sensitive quantity, matches well of first and second moment.
- Topological charge correlator $\langle q(n_t) q(0) \rangle$ and glueball mass.
- Critical slowdown, which makes transitioning to a new, independent configuration difficult. This inhibits the gathering of statistics, and helps us explain why we for larger β values have fewer independent gauge configurations.

Conclusion

- Created a code capable of generating and flowing gauge configurations.
  - Verified to match other code bases down to machine precision.
- t_0 and w_0 match other papers, e.g. Lüscher [2010] and Cè et al. [2015].
- $\langle Q \rangle \neq 0$ for some ensembles.
- The topological susceptibility $\left\langle \chi_f^{1/4} \right\rangle$ and N_f
- $\left\langle Q^4 \right\rangle_C$ and R. Sensitive quantities - need large statistics.
- Topological charge correlator $\langle q(n_t) q(0) \rangle$ and glueball mass.
- Statistics, autocorrelation and critical slowdown.

- Checked scaling and parameter optimization.
- Same results as Chroma down to machine precision.
- t_0 and w_0 match other papers.
- $\langle Q \rangle$
- $\chi_f^{1/4}$. Matches well with other papers
- $\left\langle Q^4 \right\rangle_C$ and R. Sensitive quantity, matches well of first and second moment.
- Topological charge correlator $\langle q(n_t) q(0) \rangle$ and glueball mass.
- Critical slowdown, which makes transitioning to a new, independent configuration difficult. This inhibits the gathering of statistics, and helps us explain why we for larger β values have fewer independent gauge configurations.

Future developments and final thoughts

- Better statistics - more gauge configurations.

Future developments and final thoughts

- Better statistics - more gauge configurations.
- Implement better actions with operators that has smaller error contributions.

Future developments and final thoughts

- Better statistics - more gauge configurations.
- Implement better actions with operators that has smaller error contributions.
- Fermions and HMC(Hybrid Monte Carlo).

Questions?

References

S. Borsanyi, S. Durr, Z. Fodor, C. Hoelbling, S. D. Katz, S. Krieg, T. Kurth, L. Lellouch, T. Lippert, C. McNeile, and K. K. Szabo. High-precision scale setting in lattice QCD. *Journal of High Energy Physics*, 2012(9), September 2012. ISSN 1029-8479. doi: 10.1007/JHEP09(2012)010. URL http://arxiv.org/abs/1203.4469. arXiv: 1203.4469.

Marco Cè, Cristian Consonni, Georg P. Engel, and Leonardo Giusti. Non-Gaussianities in the topological charge distribution of the SU(3) Yang–Mills theory. *Physical Review D*, 92(7), October 2015. ISSN 1550-7998, 1550-2368. doi: 10.1103/PhysRevD.92.074502. URL http://arxiv.org/abs/1506.06052. arXiv: 1506.06052.

Martin Lüscher. Properties and uses of the Wilson flow in lattice QCD. *Journal of High Energy Physics*, 2010(8), August 2010. ISSN 1029-8479. doi: 10.1007/JHEP08(2010)071. URL http://arxiv.org/abs/1006.4518. arXiv: 1006.4518.

Hans Munthe-Kaas. Runge-Kutta methods on Lie groups. *BIT Numerical Mathematics*, 38(1):92–111, March 1998. ISSN 0006-3835, 1572-9125. doi: 10.1007/BF02510919. URL http://link.springer.com/10.1007/BF02510919.

Extra slides

Scaling

We checked three types of scaling,

- **Strong scaling:** *fixed problem* and a *variable N_p cores*

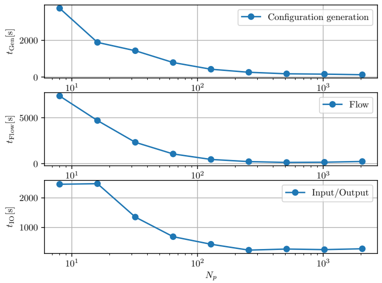

- Strong scaling

Scaling

We checked three types of scaling,

- **Strong scaling:** *fixed problem* and a *variable N_p cores*
- **Weak scaling:** *fixed problem per processor* and a *variable N_p cores.*

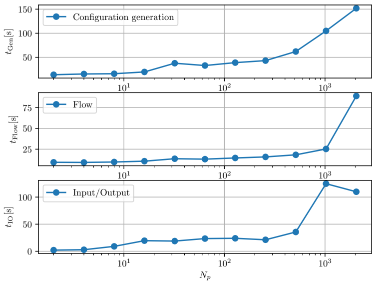

- Strong scaling
- Weak scaling

Scaling

We checked three types of scaling,

- **Strong scaling:** *fixed problem* and a *variable N_p cores*
- **Weak scaling:** *fixed problem per processor* and a *variable N_p cores.*
- **Speedup:** defined as $S(p) = \frac{t_{N_p}}{t_{N_p,0}}$.

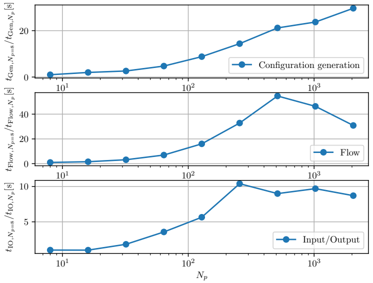

- Strong scaling
- Weak scaling
- The speedup of the configuration generation, flowing, and IO. The speedup is calculated by dividing the run time of each N_p run, with the run time of the run with the least number of processors, $N_p = 8$.

Scaling

We checked three types of scaling,

- **Strong scaling:** *fixed problem* and a *variable N_p cores*
- **Weak scaling:** *fixed problem per processor* and a *variable N_p cores*.
- **Speedup:** defined as $S(p) = \frac{t_{N_p}}{t_{N_p,0}}$.

- Strong scaling
- Weak scaling
- The speedup of the configuration generation, flowing, and IO. The speedup is calculated by dividing the run time of each N_p run, with the run time of the run with the least number of processors, $N_p = 8$.
- The IO was optimized later to be a factor of ten or more faster.

Scaling

We checked three types of scaling,

- **Strong scaling:** *fixed problem* and a *variable N_p cores*
- **Weak scaling:** *fixed problem per processor* and a *variable N_p cores*.
- **Speedup:** defined as $S(p) = \frac{t_{N_p}}{t_{N_p,0}}$.

We appear to have a plateau around 512 cores.

- Strong scaling
- Weak scaling
- The speedup of the configuration generation, flowing, and IO. The speedup is calculated by dividing the run time of each N_p run, with the run time of the run with the least number of processors, $N_p = 8$.
- The IO was optimized later to be a factor of ten or more faster.

Optimizing the gauge configuration generation

Generated 200 configurations for a lattice of size $N^3 \times N_T = 16^3 \times 32$ and $\beta = 6.0$, for combinations of $N_{\text{corr}} \in [200, 400, 600]$ and $N_{\text{up}} \in [10, 20, 30]$.

- We run for different values for N_{up} and N_{corr} to see what gives optimizes **computational cost** and **autocorrelation**.
- The integrated autocorrelation time for topological charge $\langle Q \rangle$ for a lattice of size $N = 16$ and $N_T = 32$ with $\beta = 6.0$ for combinations of $N_{\text{corr}} \in [200, 400, 600]$ and $N_{\text{up}} \in [10, 20, 30]$, plotted against flow time $\sqrt{8t_f}$.

Optimizing the gauge configuration generation

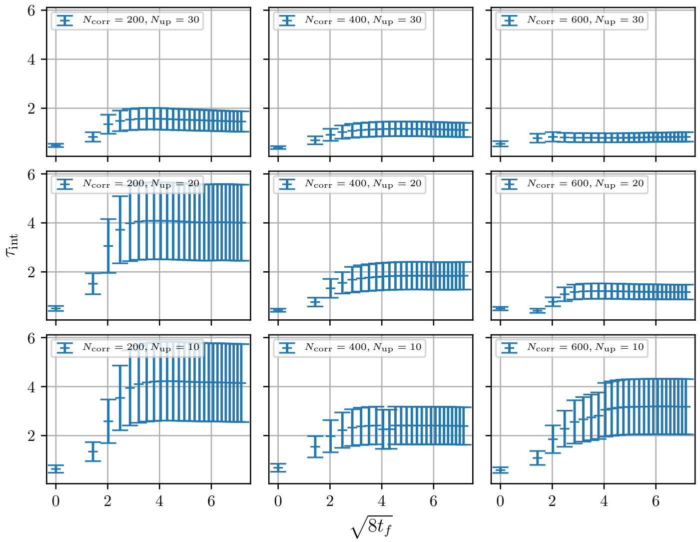

- We run for different values for N_{up} and N_{corr} to see what gives optimizes **computational cost** and **autocorrelation**.
- The integrated autocorrelation time for topological charge $\langle Q \rangle$ for a lattice of size $N = 16$ and $N_T = 32$ with $\beta = 6.0$ for combinations of $N_{\mathrm{corr}} \in [200, 400, 600]$ and $N_{\mathrm{up}} \in [10, 20, 30]$, plotted against flow time $\sqrt{8t_f}$.
- The time taking to generate 200 configurations and flowing them $N_{\mathrm{flow}} = 250$ flow steps for a lattice of size $N = 16$ and $N_T = 32$, with $\beta = 6.0$ for combinations of $N_{\mathrm{corr}} \in [200, 400, 600]$ and $N_{\mathrm{up}} \in [10, 20, 30]$.

Optimizing the gauge configuration generation

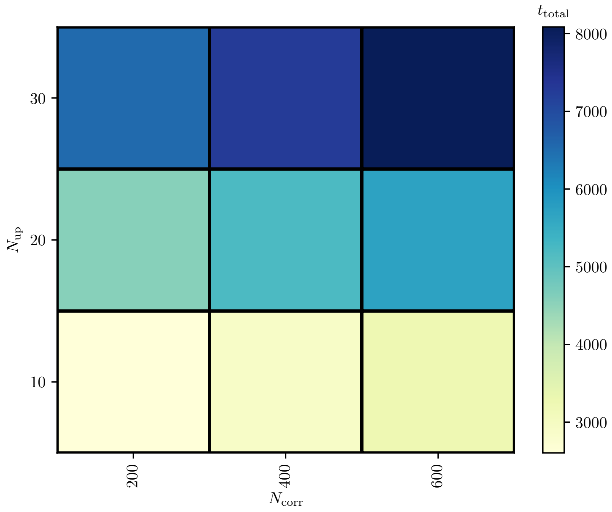

- We run for different values for N_{up} and N_{corr} to see what gives optimizes **computational cost** and **autocorrelation**.
- The integrated autocorrelation time for topological charge $\langle Q \rangle$ for a lattice of size $N = 16$ and $N_T = 32$ with $\beta = 6.0$ for combinations of $N_{\mathrm{corr}} \in [200, 400, 600]$ and $N_{\mathrm{up}} \in [10, 20, 30]$, plotted against flow time $\sqrt{8t_f}$.
- The time taking to generate 200 configurations and flowing them $N_{\mathrm{flow}} = 250$ flow steps for a lattice of size $N = 16$ and $N_T = 32$, with $\beta = 6.0$ for combinations of $N_{\mathrm{corr}} \in [200, 400, 600]$ and $N_{\mathrm{up}} \in [10, 20, 30]$.
- What we see is that increasing N_{up} is a cheaper alternative compared to using N_{corr}

Optimizing the gauge configuration generation

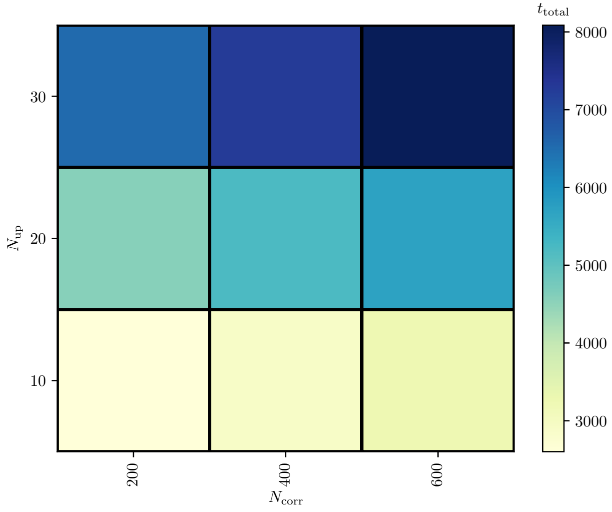

- We run for different values for N_{up} and N_{corr} to see what gives optimizes **computational cost** and **autocorrelation**.
- The integrated autocorrelation time for topological charge $\langle Q \rangle$ for a lattice of size $N = 16$ and $N_T = 32$ with $\beta = 6.0$ for combinations of $N_{\text{corr}} \in [200, 400, 600]$ and $N_{\text{up}} \in [10, 20, 30]$, plotted against flow time $\sqrt{8t_f}$.
- The time taking to generate 200 configurations and flowing them $N_{\text{flow}} = 250$ flow steps for a lattice of size $N = 16$ and $N_T = 32$, with $\beta = 6.0$ for combinations of $N_{\text{corr}} \in [200, 400, 600]$ and $N_{\text{up}} \in [10, 20, 30]$.
- What we see is that increasing N_{up} is a cheaper alternative compared to using N_{corr}

Verifying the code

- **Unit testing.** $\mathrm{SU}(3)$, $\mathrm{SU}(2)$ multiplications.

Verifying the code

- **Unit testing.** $\mathrm{SU}(3)$, $\mathrm{SU}(2)$ multiplications.
- **Integration testing.** Random matrix generation, lattice objects, parallelization, ect.

Verifying the code

- **Unit testing.** $\mathrm{SU}(3)$, $\mathrm{SU}(2)$ multiplications.
- **Integration testing.** Random matrix generation, lattice objects, parallelization, ect.
- **Validation testing.** Cross checking results with a configuration from Chroma.

Verifying the integration

Testing the integrator for different integration steps ϵ_f.

ϵ_f	0.001	0.005	0.007	0.009	0.01	0.02	0.03	0.05	0.1	0.5

- The values we will test the integrator against.

Verifying the integration

Lattice size $N^3 \times N_T = 24^3 \times 48$ with $\beta = 6.0$.

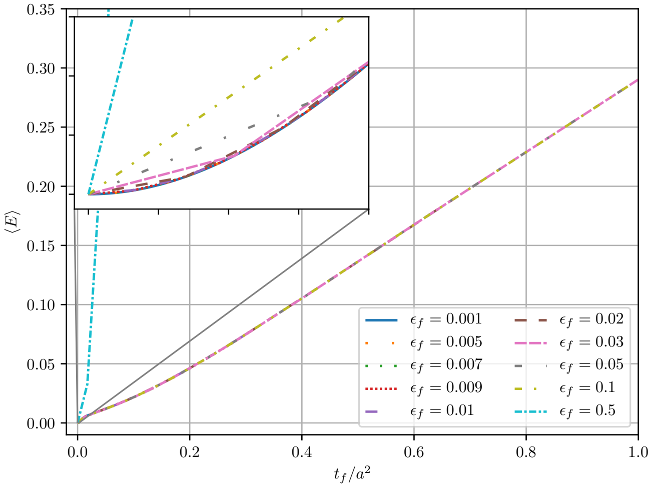

- The values we will test the integrator against.
- The energy flowed for different the different ϵ_f values.

Verifying the integration

The absolute difference between the smallest flow time $\epsilon_f = 0.001$ and those shown previously.

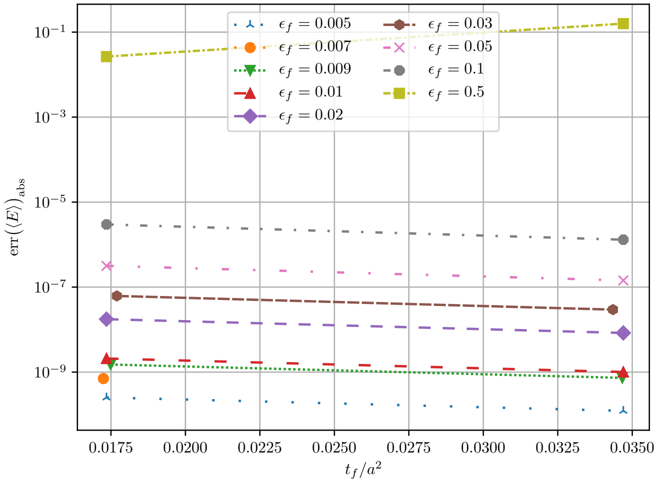

- The values we will test the integrator against.
- The energy flowed for different the different ϵ_f values.
- The absolute difference between the smallest flow time $\epsilon_f = 0.001$ and those listed in previous table.
- The reason for **only having two points** is due to the fact that we are only **comparing points** that are **close to each other in flow time**. If we were to have more points, we would have to double the number of flow time steps for the smallest lattices.

Verifying the integration

The absolute difference between the smallest flow time $\epsilon_f = 0.001$ and those shown previously.

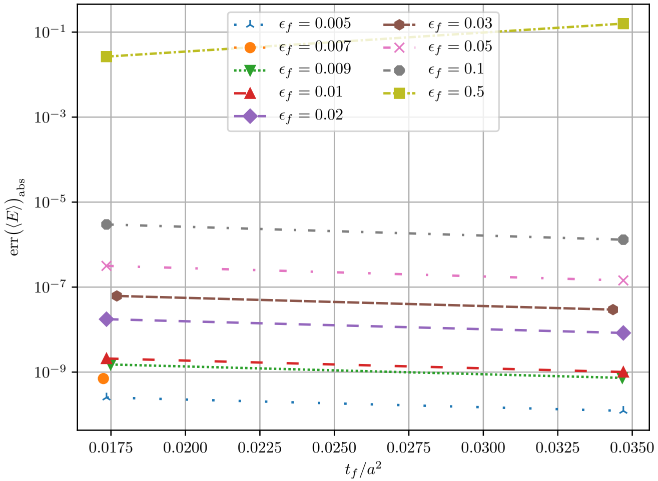

- The values we will test the integrator against.
- The energy flowed for different the different ϵ_f values.
- The absolute difference between the smallest flow time $\epsilon_f = 0.001$ and those listed in previous table.
- The reason for **only having two points** is due to the fact that we are only **comparing points** that are **close to each other in flow time**. If we were to have more points, we would have to double the number of flow time steps for the smallest lattices.
- An **example** of the flowing, can be seen by observing the **energy evolving over flow time**.

Verifying the integration

The absolute difference between the smallest flow time $\epsilon_f = 0.001$ and those shown previously.

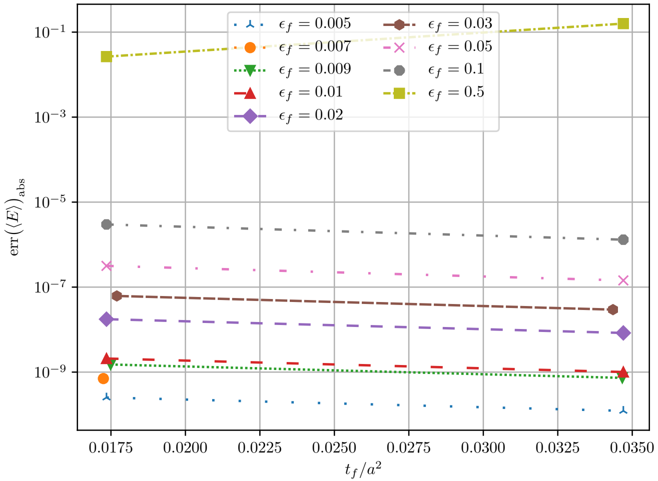

- The values we will test the integrator against.
- The energy flowed for different the different ϵ_f values.
- The absolute difference between the smallest flow time $\epsilon_f = 0.001$ and those listed in previous table.
- The reason for **only having two points** is due to the fact that we are only **comparing points** that are **close to each other in flow time**. If we were to have more points, we would have to double the number of flow time steps for the smallest lattices.
- An **example** of the flowing, can be seen by observing the **energy evolving over flow time**.

The non-linearity of QCD

The QCD Lagrangian

$$\mathcal{L}_{\mathrm{QCD}} = \sum_{f=1}^{N_f} \bar{\psi}^{(f)} \left(i\not{D} - m^{(f)} \right) \psi^{(f)} - \frac{1}{4} G^a_{\mu\nu} G^{a\mu\nu},$$

with action

$$S = \int \mathrm{d}^4 x \mathcal{L}_{\mathrm{QCD}}, \tag{1}$$

is invariant under a $\mathrm{SU}(3)$ symmetry.

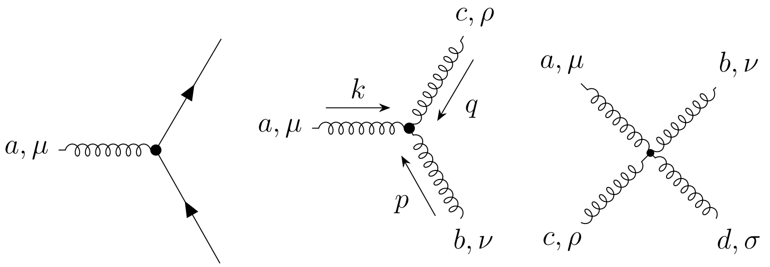

- *Gluon self-interaction.*
- This central aspect is mostly covered in the pure-gauge/Yang-Mills section of the theory.
- **Two important features**: *confinement* and *asymptotic freedom*.

Asymptotic freedom

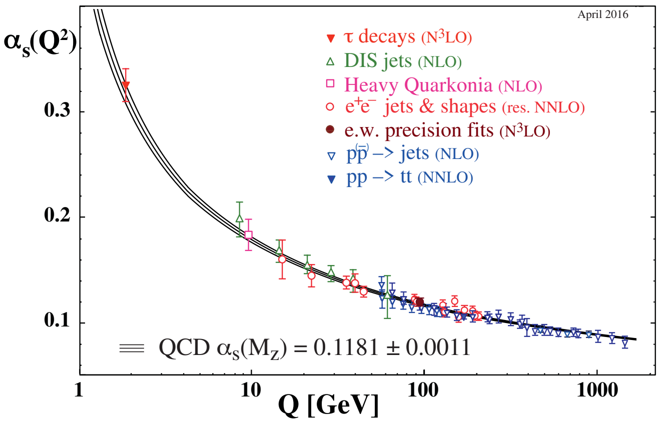

- The coupling constant **decreases** as we **increase** the energy.
- Also serves as an *experimental proof* of QCD.
- Other lines of *evidence*: triple γ decay and muon cross section ratio R.
  - Triple γ decay: the number of colors is included in the cross section, which can be measured experimentally.
  - Muon cross section ratio R: the ratio is dependent on having three colors.

Solving gradient flow with Runge-Kutta 3

With

$$\dot{V}_{t_f} = -g_S^2 \left\{\partial_{x,\mu} S_G[V_{t_f}]\right\} V_{t_f} = Z(V_{t_f}) V_{t_f},$$

- We rewrite the equations slightly,

Solving gradient flow with Runge-Kutta 3

With

$$\dot{V}_{t_f} = -g_S^2 \left\{\partial_{x,\mu} S_G[V_{t_f}]\right\} V_{t_f} = Z(V_{t_f}) V_{t_f},$$

and $Z_i = \epsilon_f Z(W_i)$ we get

$$\begin{aligned}
W_0 &= V_{t_f}, \\
W_1 &= \exp\left[\frac{1}{4} Z_0\right] W_0, \\
W_2 &= \exp\left[\frac{8}{9} Z_1 - \frac{17}{36} Z_0\right] W_1, \\
V_{t_f+\epsilon_f} &= \exp\left[\frac{3}{4} Z_2 - \frac{8}{9} Z_1 + \frac{17}{36} Z_0\right] W_2,
\end{aligned}$$

with coefficients from Lüscher [2010].

- We rewrite the equations slightly,
- and use a structure preserving integrator with coefficients from Lüscher [2010].

Solving gradient flow with Runge-Kutta 3

With

$$\dot{V}_{t_f} = -g_S^2 \left\{\partial_{x,\mu} S_G[V_{t_f}]\right\} V_{t_f} = Z(V_{t_f}) V_{t_f},$$

and $Z_i = \epsilon_f Z(W_i)$ we get

$$\begin{aligned} W_0 &= V_{t_f}, \\ W_1 &= \exp\left[\frac{1}{4} Z_0\right] W_0, \\ W_2 &= \exp\left[\frac{8}{9} Z_1 - \frac{17}{36} Z_0\right] W_1, \\ V_{t_f+\epsilon_f} &= \exp\left[\frac{3}{4} Z_2 - \frac{8}{9} Z_1 + \frac{17}{36} Z_0\right] W_2, \end{aligned}$$

with coefficients from Lüscher [2010].

- We rewrite the equations slightly,
- and use a structure preserving integrator with coefficients from Lüscher [2010].
- We control the accuracy of this integrator by ϵ_f.

Solving gradient flow with Runge-Kutta 3

With

$$\dot{V}_{t_f} = -g_S^2 \left\{ \partial_{x,\mu} S_G[V_{t_f}] \right\} V_{t_f} = Z(V_{t_f}) V_{t_f},$$

and $Z_i = \epsilon_f Z(W_i)$ we get

$$\begin{aligned} W_0 &= V_{t_f}, \\ W_1 &= \exp\left[\frac{1}{4} Z_0\right] W_0, \\ W_2 &= \exp\left[\frac{8}{9} Z_1 - \frac{17}{36} Z_0\right] W_1, \\ V_{t_f+\epsilon_f} &= \exp\left[\frac{3}{4} Z_2 - \frac{8}{9} Z_1 + \frac{17}{36} Z_0\right] W_2, \end{aligned}$$

with coefficients from Lüscher [2010].

- We rewrite the equations slightly,
- and use a structure preserving integrator with coefficients from Lüscher [2010].
- We control the accuracy of this integrator by ϵ_f.

Additional ensembles

Ensemble	N	N_T	N_{cfg}	N_{corr}	N_{up}	a [fm]	L [fm]
E	8	16	8135	600	30	0.0931(4)	0.745(3)
F	12	24	1341	200	20	0.0931(4)	1.118(5)
G	16	32	2000	400	20	0.0790(3)	1.265(6)

- Additional ensembles made in order to illuminate additional aspects of the topological charge.
- Supporting ensembles made on Smaug. All ensembles were flown $N_{\mathrm{flow}} = 1000$ steps with $\epsilon_{\mathrm{flow}} = 0.01$.

Energy definition

Some people use a banana for scale

- Defined as the field strength tensor squared averaged over all lattice points and directions.

Energy definition

We use t_0

$$E = \frac{a^4}{2|\Lambda|} \sum_{n\in\Lambda} \sum_{\mu,\nu} \left(F^{\text{clov}}_{\mu\nu}(n)\right)^2$$

- Defined as the field strength tensor squared averaged over all lattice points and directions.
- We will use the clover field strength definition in gauge observables.
- **Symmetries** will allow us to **reduce** the effective **number of clovers** need to **calculate from 24 to 6**.

Energy definition

We use t_0

$$E = \frac{a^4}{2|\Lambda|} \sum_{n\in\Lambda} \sum_{\mu,\nu} \left(F_{\mu\nu}^{\text{clov}}(n)\right)^2$$

$F_{\mu\nu}^{\text{clov}}(n)$ is given by

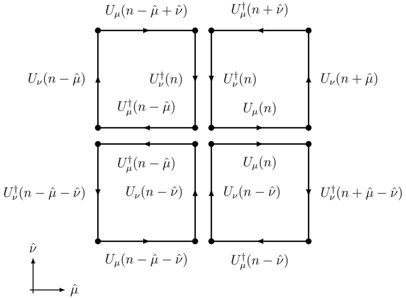

- Defined as the field strength tensor squared averaged over all lattice points and directions.
- We will use the clover field strength definition in gauge observables.
- **Symmetries** will allow us to **reduce** the effective **number of clovers** need to **calculate from 24 to 6**.

Energy

Using scale definition t_0 from Lüscher [2010],

$$\left\{ t_f^2 \left\langle E(t) \right\rangle \right\}_{t_f = t_0} = 0.3.$$

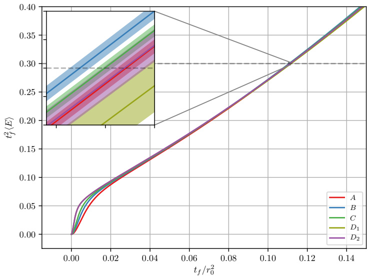

Scale setting t_0

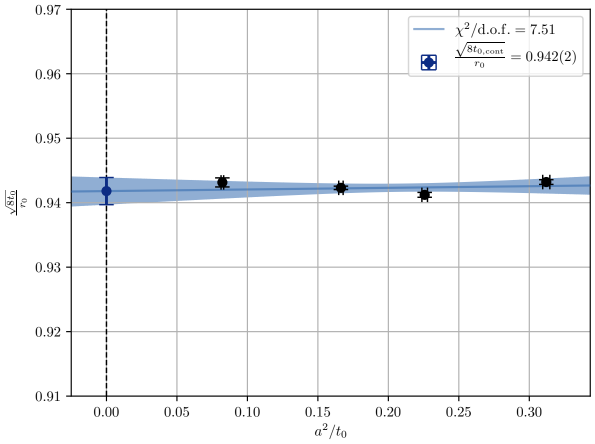

Continuum extrapolation using ensembles A, B, C, and D_2 gives $t_{0,\text{cont}}/r_0^2 = 0.11087(50)$.

- The continuum extrapolation $a \to 0$ for t_0 of the four ensembles A, B, C, and D_2.
-

Scale setting t_0

This matches the values retrieved by Lüscher [2010],

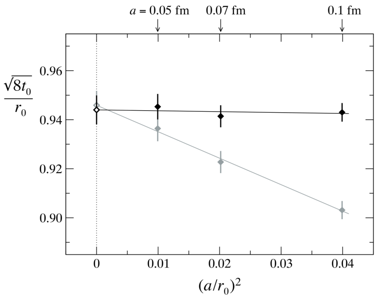

- The continuum extrapolation $a \to 0$ for t_0 of the four ensembles A, B, C, and D_2.
- $r_0 = 0.5$ fm.

Scale setting t_0

This matches the values retrieved by Lüscher [2010],

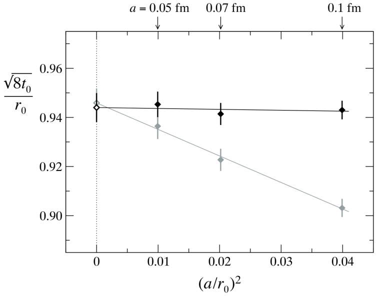

- The continuum extrapolation $a \to 0$ for t_0 of the four ensembles A, B, C, and D_2.
- $r_0 = 0.5$ fm.

Scale setting t_0

Extrapolations for different ensemble-combinations

Ensembles	$t_{0,\mathrm{cont}}/r_0^2$	$\chi^2/\mathrm{d.o.f}$
A, B, C, D_2	$0.11087(50)$	7.51
B, C, D_2	$0.1115(3)$	0.41
A, B, C, D_1	$0.1119(6)$	0.88

- Notice the χ^2/d.o.f. of the extrapolation versus the two other extrapolations.

Scale setting w_0

Can also set a scale using the derivative which offers more granularity for small flow times,

$$W(t)|_{t=w_0^2} = 0.3,$$

$$W(t) \equiv t_f \frac{\mathrm{d}}{\mathrm{d}t_f} \left\{ t_f^2 \langle E \rangle \right\}.$$

First presented by Borsanyi et al. [2012].

Scale setting w_0

Ensembles	$w_{0,\mathrm{cont}}$[fm]	$\chi^2/\mathrm{d.o.f}$
A, B, C, D_2	$0.1695(5)$	7.12
B, C, D_2	$0.1702(3)$	0.53
A, B, C, D_1	$0.1706(6)$	0.86

Scale setting w_0

Ensembles	$w_{0,\text{cont}}$[fm]	$\chi^2/\text{d.o.f}$
A, B, C, D_2	$0.1695(5)$	7.12
B, C, D_2	$0.1702(3)$	0.53
A, B, C, D_1	$0.1706(6)$	0.86

Comparable to Borsanyi et al. [2012] which included dynamical fermions, with $w_{0,\text{cont}} = 0.1755(18)(04)$ fm.